MINISTÈRE
DES ARMÉES
Liberté
Égalité
Fraternité

Direction générale
de l'armement

DGA Techniques aérospatiales

TECHNICAL REPORT

REVIEW OF AERONAUTICAL FATIGUE INVESTIGATIONS IN FRANCE DURING THE PERIOD JUNE 2023- JUNE 2025

N° 25-DGATA-ST-ICAF_2025-V1F

MINISTÈRE
DES ARMÉES
Liberté
Égalité
Fraternité

Direction générale
de l'armement

DIRECTION DE L'INGÉNIERIE ET DE L'EXPERTISE

DGA Aerospace Systems

Division Structures

Your contact : TOUZET Laurent

REVIEW OF AERONAUTICAL FATIGUE INVESTIGATIONS IN FRANCE DURING THE PERIOD JUNE 2023- JUNE 2025

TECHNICAL NOTE

N° 25-DGATA-ST-ICAF_2025-V1F

	NAME Surname	Visa	Date	Title
Prepared by	TOUZET Laurent		15/03/2025	Technical referent for aeronautical structure

Direction générale de l'armement

DGA Techniques aérospatiales

47 rue Saint-Jean - CS n° 93123 - 31131 BALMA Cedex

Téléphone : +33 (0)5.62.57.57.57

Table of contents

TABLE OF CONTENTS

****

Direction générale de l'armement

DGA Techniques aérospatiales

47 rue Saint-Jean - CS n° 93123 - 31131 BALMA Cedex

Téléphone : +33 (0)5.62.57.57.57 – Télécopie : +33 (0)5.62.57.54.47

0. Introduction and thanks

The present review, prepared to be published online on ICAF website, summarizes works performed in France in the field of aeronautical fatigue and structural integrity, over the period June 2023 - June 2025.

Subjects are grouped by themes addressed at the ICAF. The list of themes is presented below:

- 1- Fatigue crack growth and life prediction methods
- 2- Structural integrity of composite structures
- 3- Full-scale fatigue testing
- 4- Sustainable aviation
- 5- Reliability and risk-analysis of structures and mechanisms
- 6- Advanced materials and innovative structural concepts
- 7- Fatigue life enhancement methods and repair solutions
- 8- NDI inspections and structural load/health monitoring

Article contributors are listed below the article title. Many thanks to all of them for their contribution.

1. Fatigue crack growth and life prediction methods

1.1. Fatigue crack growth simulation with ABAQUS

Contact: Mme BAUBRY Emeline (DGA TA)

1.1.1. Introduction

This work is included in a global study on prediction of fatigue crack growth in metallic parts called IFIP (Fatigue Index, Growth Index). The IFIP study aims to develop a tool to predict a crack growth based on a part's geometry and material and a cyclic loading. This tool partly relies on the Finite Element simulations of fatigue crack growth with the software ABAQUS. Two types of output can be obtained from the FE models:

- The crack propagation visualization within the ABAQUS CAE.
- Stress intensity factor at the crack tip versus crack length curve.

The latter output is an essential input to estimate the crack growth with other crack propagation laws such as the Elber law, the Preffas or the Onera method. However, ABAQUS crack growth calculations are realized with energetic values such as the energy release rate. Thus Irwin formula is used to obtain stress intensity factor from energy release rate.

Pre-craked parts of various geometries and materials went under cycling loading simulations. In order to explore the abilities of ABAQUS, simulations in 2D, 3D and with residual stress fields have been realized. For all simulations presented in this article, cracks are modelled with the eXtended Finite Element Method (XFEM) and crack growth is defined by the material Paris law. To perform cycling loading, ABAQUS relies on a linear elastic fatigue crack growth analysis thus material is simply defined by an elastic behaviour. This combination of techniques models crack propagation of a discrete crack along an arbitrary path without remeshing.

Models with residual stress field requires a first simulation of the test used to introduce stress field. For this simulation, material plastic behaviour and/or thermal behaviour is defined.

1.1.2. CT specimen

The CT specimen is perfectly suited to perform controlled crack growth. Thanks to the countless studies on the matter, an analytical formula for stress intensity factor vs. crack length has been developed. Thus, this formula can be used to evaluate the crack propagation method used in ABAQUS.

A constant amplitude loading fatigue is applied with a stress ratio R = 0.1. Maximal stress for fatigue loading is chosen to ensure crack growth but it must not be high enough to generate plasticity in other areas than crack tip.

In light of the loading and material properties, Paris law is valid on the following range of crack length a: 32 mm < a < 55 mm. Thus simulation outputs are only analyzed on this crack length range.

1.1.3. 2D CT specimen

Crack growth in 2D CT specimen was simulated with 2 initial configurations:

- Conf. 1: Basic CT specimen without any residual stress field.
- Conf. 2: CT specimen with residual stress field induced by lateral compression.

The residual stress field induced by lateral compression is shown Figure 1. Regarding crack length range considered, the residual stress along Y in this area is slightly positive, around a few MPa.

Figure 2 shows stress intensity factor vs. crack length curves for both configurations. Basic 2D CT model displays satisfying results regarding the analytical results. Results are highly sensitive to elements aspect ratio thus a special attention must be paid to the mesh definition in the crack growth area.

Although residual stress field values are low, stress intensity factor has decreased overall in the propagation area. This decrease greatly impacts the crack growth with a significant propagation slow down: the final crack length (55mm) is reached after 160000 cycles with the residual stress field whereas the basic CT specimen reaches it after 110000 cycles.

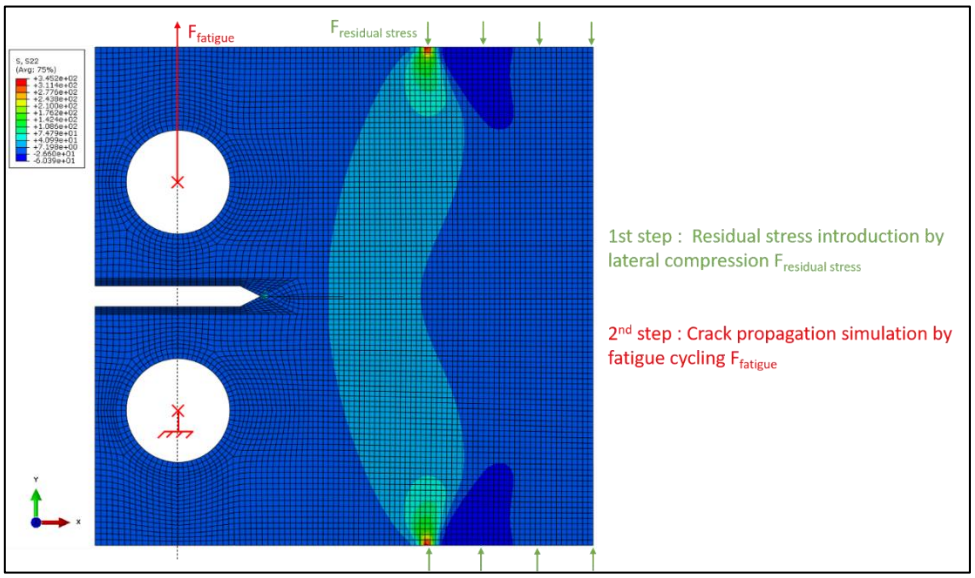

Figure 1: Residual stress field introduced in the 2D CT model

1.1.4. 3D CT specimen

3D CT specimen crack growth was simulated without any residual stress field. Since there are multiple elements along the specimen thickness, for a step analysis increment, there are multiple crack length values and multiple stress intensity factor values. This is not an issue for the 2D case since there is only one element to model the specimen thickness hence a single element at the crack tip. Thus, 2D results can be used as a comparison with the 3D results to validate the method used to estimate a single crack length and a single stress intensity factor for each step analysis increment in the 3D simulation.

Calculating crack lengths mean and stress intensity factors mean along the specimen thickness seems to be the most accurate method. Stress intensity factor vs crack length curve is shown Figure 2. Mesh definition in the X-Y plane is the same for 2D and 3D simulations. Difference between 2D and 3D stress intensity factor for a crack length is less than 0.01 MPa.m1/2. However, this small gap is enough to induce a few thousands cycles gap at a = 55 mm.

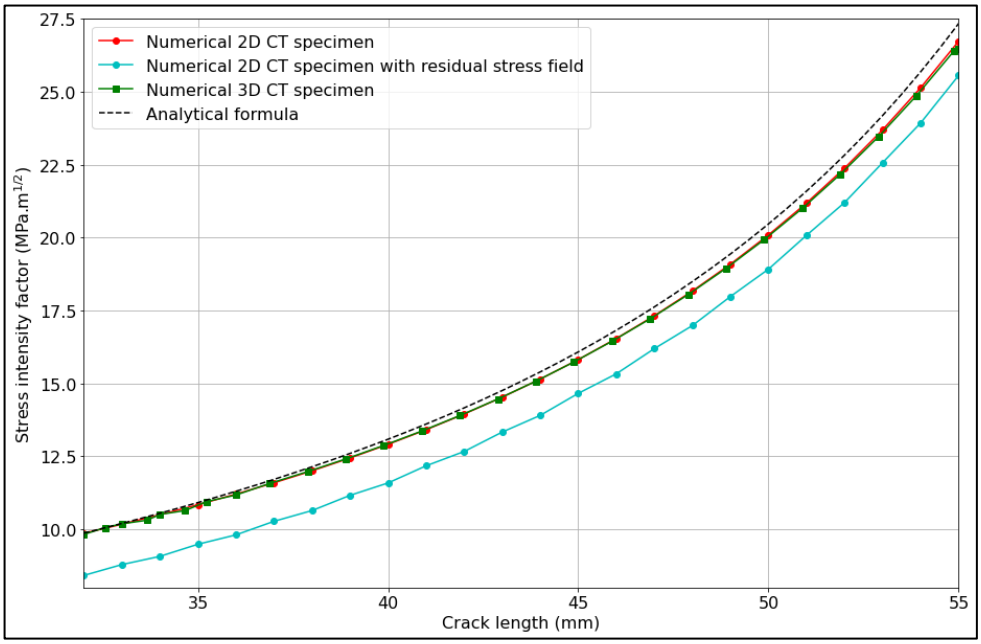

Figure 2: 2D and 3D CT specimen stress intensity factor vs. crack length curves

1.1.5. Wing beam specimen

This specimen represents a simplified wing beam. It was designed for the IFIP study as a more complex part yet with an easily predictable crack path. Figure 3 shows the beam geometry: threads on the X-Y plane allows to attach the wing skin to the beam. A pre-crack is introduced on a thread edge, circled in red on Figure 3. Red mesh elements are the pre-cracked ones. Mesh is particularly refined in the crack propagation area, between the thread and the beam edge.

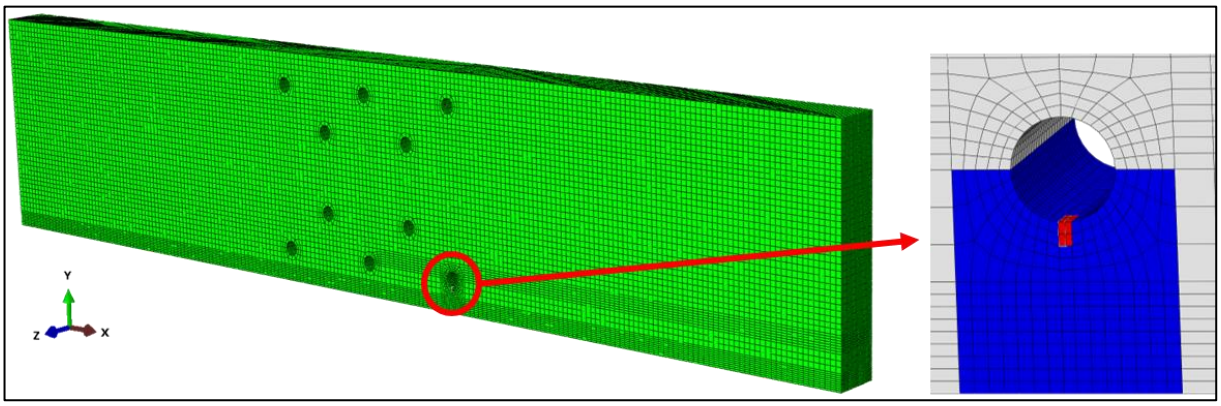

Figure 3: Beam specimen geometry and mesh

The specimen is subjected to uniaxial tensile load in the X direction. The load follows a constant amplitude fatigue loading with a stress ratio R = 0.1. Thus mode I rupture is predominant. The crack mainly grows along a Y-Z surface. A critical propagation direction is chosen: crack length "a" is defined as the crack length along the thread. Since beam thickness is 25 mm, crack propagation is studied for crack length a between 1 mm (pre-crack dimension) and 25 mm (beam entirely cracked along thread).

Fatigue crack propagation tests were conducted on this specimen. Their results can be used as a means of validation for simulation results. This case is also an opportunity to compare other propagation prediction methods such as the Elber law, the ONERA method, the Nasgros method and the PREFFAS method. Comparisons are shown Figure 4.

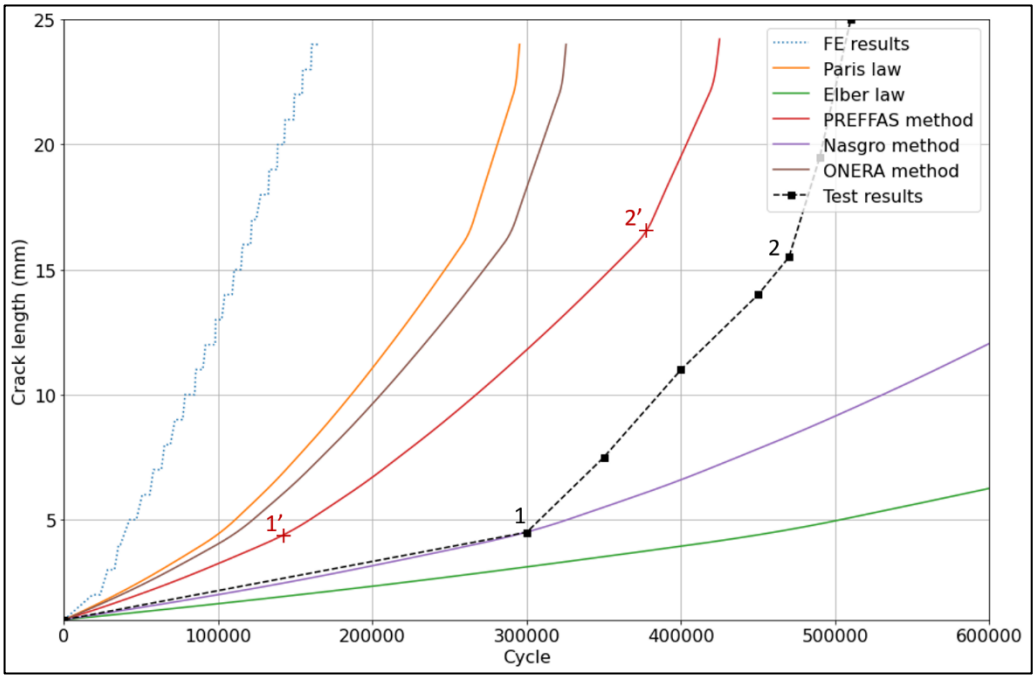

Figure 4: Wing beam specimen's crack propagation predictions with different methods

FE results curve is a direct plot of the ABAQUS crack propagation. Continuous lines are the crack propagation results from ABAQUS stress intensity factor applied to other propagation prediction methods. As mentioned above, crack growth in ABAQUS is based on Paris law. However, there is a significant difference with the Paris law curve. Direct crack propagation estimations from ABAQUS have to be carefully considered.

In this specific case, PREFFAS method seems to be the most adequate one but remaining gaps with test results are still large. Test results curve has inflection points: point 1 (a ≈ 4.5mm) and point 2 (a ≈ 15.5 mm). These inflection points are clearly visible on the Paris, ONERA and PREFFAS curves which is encouraging: even if the FE life prediction is not really accurate, physical phenomena are represented. A trial to adjust FE life prediction might be the use of multi slope propagation speed curve thus defining different material Paris coefficients depending on the stress intensity factor. In this case, the Paris coefficients used seem too conservative for the low stress intensity factor values thus for the low crack lengths (1 mm < a < 4,5 mm).

1.1.6. Welded bar specimen

This case aims at introduce residual stress field induced by thermal loading. The objective is to assess thermal manufacturing impact on residual part strength. The specimen is made from 2 bars welded together. Pre-crack is manufactured in the welded area (Figure 5). Uniaxial tensile load in Z direction will obviously contribute to mainly mode I crack propagation in a X-Y plane. The interest of this study case relies on the application of uniaxial compressive load in the Z direction.

This type of solicitation usually does not significantly contribute to crack growth. However, residual stress field induced by welding might modify enough the material properties so that the crack propagates under compressive loading. Simulation work needed to model this case is much more complex than the others. Three main tasks have been identified:

- 1st simulation: Residual stress field introduction, representative of the welding.
- 2nd simulation: Crack propagation under uniaxial tensile load in Z direction.
- 3rd simulation: Crack propagation under uniaxial compressive load in Z direction.

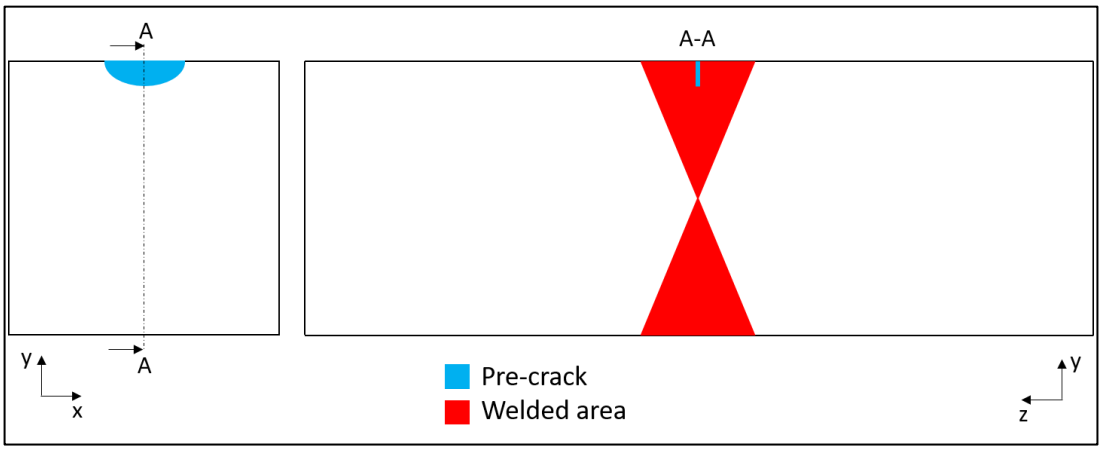

Figure 5: Welded bar drawing

This case presents many challenges. In addition to required material properties for crack propagation, the material thermal behaviour has to be identified and modelled. The manufacturing process here is really specific thus an accurate simulation is difficult to set up. A validation process for the 1st simulation must be defined.

Another challenge is mesh definition. 1st simulation output database is an input data for 2nd and 3rd simulations. Thus, all models share a common mesh. Crack propagation simulations are very sensitive to mesh definition. 1st simulation mesh must be defined while keeping in mind mesh requirements for crack propagation simulations.

Among these requirements, an element border cannot be placed on the crack location. Moreover, along the crack growth path, elements aspect ratio must be really balanced. Hexahedron elements are the most adequate elements for crack propagation. Figure 6 shows a proper mesh definition for the welded bar specimen. Only half on the specimen is represented since Y-Z plane is a symmetry plane.

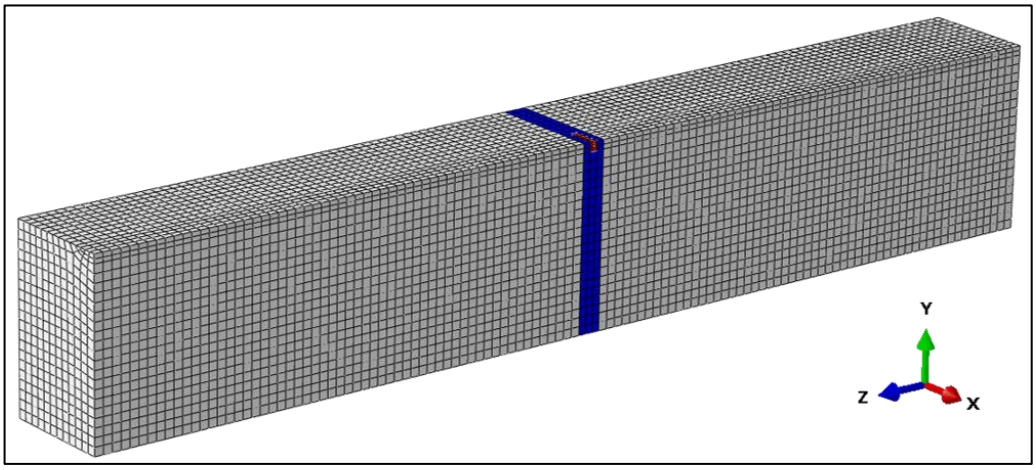

Figure 6: Welded bar FE representation and mesh

Simulations are underway, but no exploitable results are available at this time.

1.2. Upskilling of the DGTA TA materials laboratory on the characterization and modeling of HCF properties from thermometric measurements

Contacts: M. GEYER (DGA TA) / R. JACQUELIN (DGA TA) with the support of l'IRDL (Brest)

1.2.1. Context.

Polycyclic fatigue (i.e., high-cycle fatigue or HCF) is a particularly insidious aspect of the mechanical behavior of metallic materials due to its progressive and concealed nature. Although significant progress has been made since the first studies on polycyclic fatigue from the beginning of the 20th century, the design of industrial parts for high-cycle fatigue remains a major challenge. Indeed, the implementation of predictive models remains difficult mainly for three reasons:

- Fatigue behavior depends on many parameters such as the nature of the loading (e.g., load ratio, multiaxiality of the loading, loading history, etc.), the environment (temperature, etc.), the microstructure, and the manufacturing process of the part.

- Fatigue lifetimes at high cycle numbers are probabilistic in nature (i.e., a large scatter is observed on the number of cycles to fatigue failure HCF).

- Fatigue property characterization times in a given configuration with classical methods are prohibitive.

For several years, a number of research teams have been working on determining the high-cycle fatigue properties of metallic materials from self-heating tests under cyclic loading. This method proves to be very effective in reducing characterization costs and time.

It is based on the observation of the evolution of the stabilized mean temperature of a specimen subjected to a sequence of cyclic loadings by blocks. During this type of test, it is observed, once a certain amplitude level is exceeded, that the stabilized mean temperature of the specimen increases significantly.

This temperature increase is related to the fact that the fatigue limit of the material has been exceeded, giving rise to dissipative mechanisms. In reality, dissipation occurs before this value, but in a much weaker manner. An empirical exploitation of these test results shows that they allow for a rapid determination (i.e., from a single test lasting half a day and requiring only one specimen) of the endurance limit of the material.

More recently (i.e., at the dawn of the 21st century), the development of an analysis method based on a two-scale probabilistic model has shown that self-heating tests allow, with a reduced number of specimens, to estimate not only the average endurance limit of a steel, but also to predict the dispersion of the results of classical fatigue test campaigns (i.e., complete Wöhler curves).

1.2.2. Work carried out by DGA TA

Thanks to its privileged exchanges with ENSTA Bretagne and IRDL, the DGA's materials laboratory, based in Balma, wishes to develop its expertise in mastering these tests. The objective is initially to test and master the so-called "0D" technique on steel, a material on which the method has already proven its worth.

This method is suitable for homogeneous and continuous materials and is carried out through simple instrumentation by thermocouple. It contrasts with the so-called "1D" and "2D" methods which require advanced instrumentation by infrared camera, essential for the study of heterogeneous materials such as coated materials, welded joints, assemblies or complex structures.

These accelerated fatigue property evaluation methods offer several major advantages:

- Development of new materials → with the advent of new manufacturing processes with increasingly varied parameters and new alloy compositions, the number of process/material pairs is exploding, requiring rapid characterization methods.

- Maintaining operational readiness → extending the service life of equipment requires knowing how to estimate remaining service life and qualify new ad hoc repair methods. Thus, a rapid evaluation of fatigue properties from a single sample is of great interest.

- Investigation → During technical incidents in service or production, sample collection is often very limited and a strong reactivity is expected to identify the root causes

In order to assess the self-heating (SH) method for determining fatigue properties, the method was implemented at DGA TA and the results were compared to those obtained by the conventional staircase method.

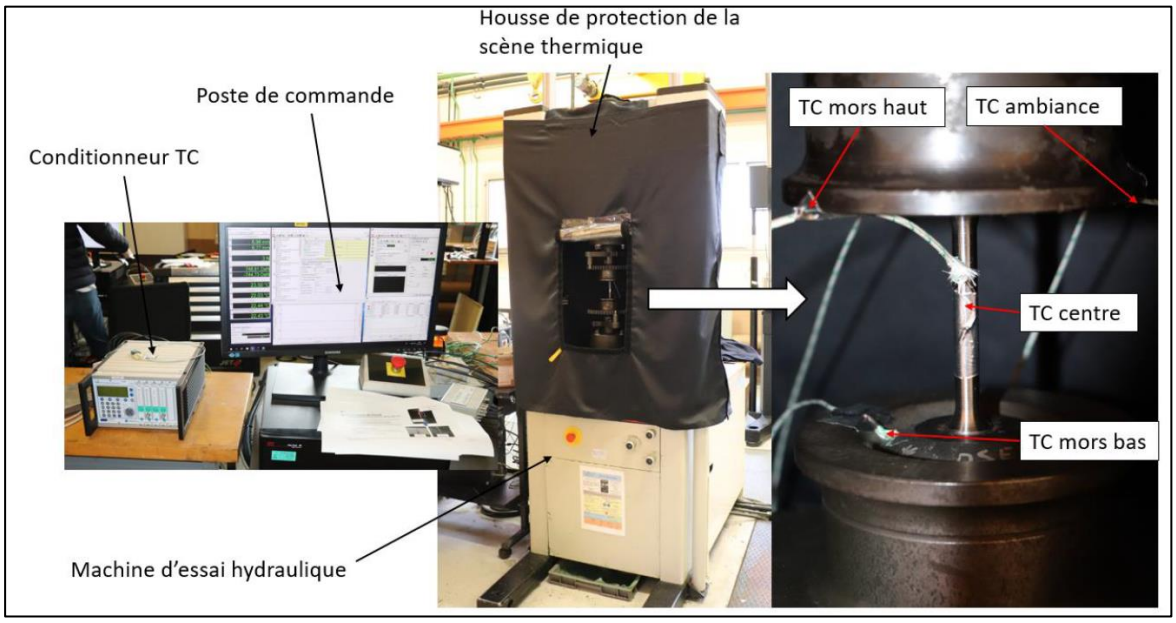

Figure 1: Experimental setup of a 0D self-heating test.

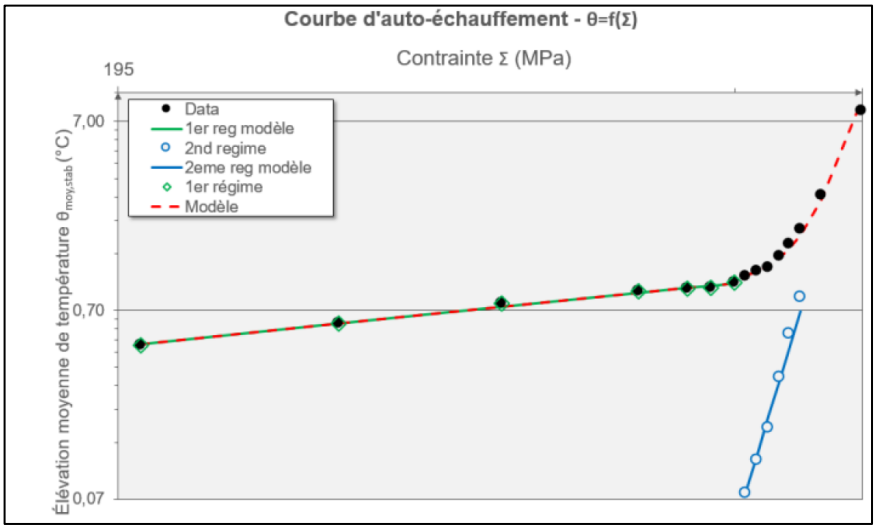

Figure 2: Example of post-processing of a self-heating test.

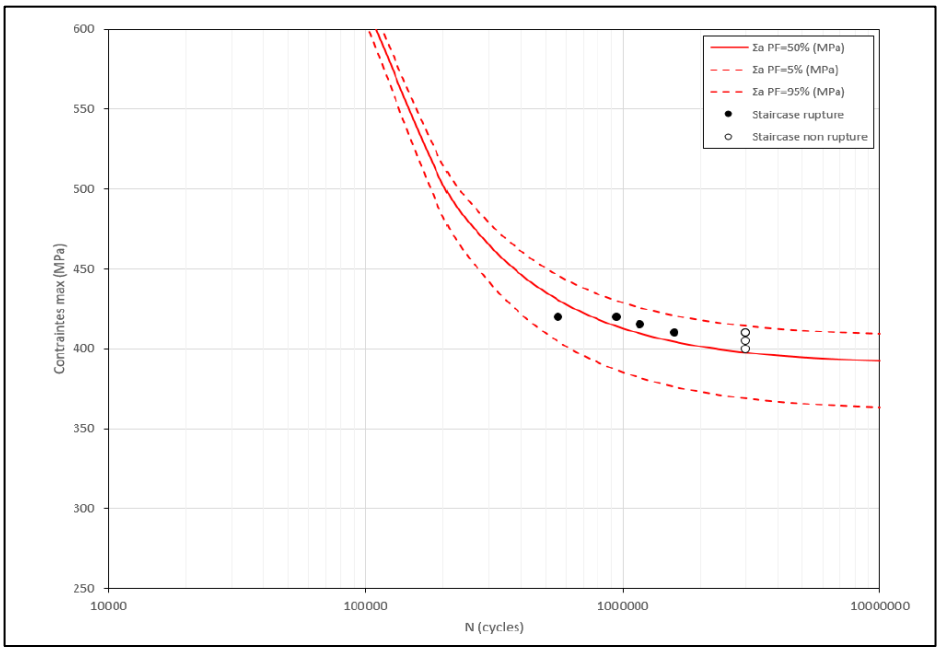

Figure 3: Comparison of SH and staircase results.

Finally, this first application of the SH method to DGA TA is very encouraging. It is an easy-to-implement method that provides satisfactory results for quickly determining the endurance limit from a few specimens. A minimum of 2 specimens seems to be required: the first to "rough out" the loading steps and the second to refine the area of interest around the endurance limit. In addition to the obvious time and cost savings compared to a staircase campaign, the ease of machining the specimens and the elimination of biases induced by it (surface condition, residual stresses, defects, etc.) improve the reliability of the results and their interpretation.

In terms of perspectives, it is planned to apply the AE 0D method to other alloys which will certainly require an adaptation of the 0D protocol. Thus, it is planned to continue the study internally on stainless steels while in parallel the IRDL is working on the application of the method on aluminum alloys. Due to their physical properties, they do not exhibit the same thermal response, which does not allow for the clear identification of two distinct regimes as is the case for steels.

2. Structural integrity of composite structures

2.1. Experimental characterization of two structural bonded composite repairs

Contact: Mame BARRIERE Nathalie (DGA TA)

2.1.1. Introduction

Structural repairs are necessary to restore the mechanical properties of damaged composite parts, including strength, durability, and damage tolerance. Common repair methods for primary structures include bolted or hybrid (bolted and bonded) repairs, as non-destructive techniques for detecting weak bonds are lacking.

Bonded repairs, however, offer benefits like weight savings and uniform load transfer. This study explores the behaviour of bonded repairs and their failure mechanisms by investigating two repair strategies on a 400 mm by 400 mm panel (Figure 1): a flush wet lay-up (WLU) repair with dry fabric and film adhesive, and an external pre-cured patch bonded with the same adhesive.

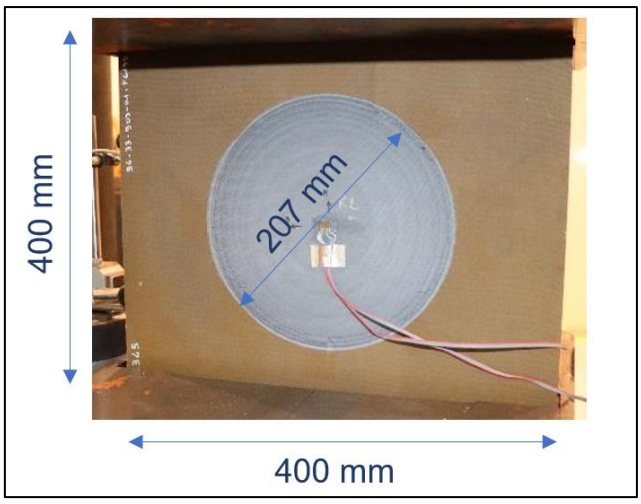

Figure 1 : Composite repaired panel

2.1.2. Experimental work

The parent composite panels were made of 24 plies of UD carbon fiber/epoxy prepreg, cured in an autoclave at 180°C. The initial damage consisted of a machined hole with a 75 mm diameter and a depth of 10 plies.

The first repair is a flush repair composed of 6 mm long steps, laid up with carbon fabric and film adhesive (Figure 2). An over-ply was added on top of the repair to provide protection and stiffness at the joint tips, as well as to reduce peak stresses. The repair was cured at 110°C using a thermal blanket and a portable device, which allowed for temperature and vacuum control throughout the entire process.

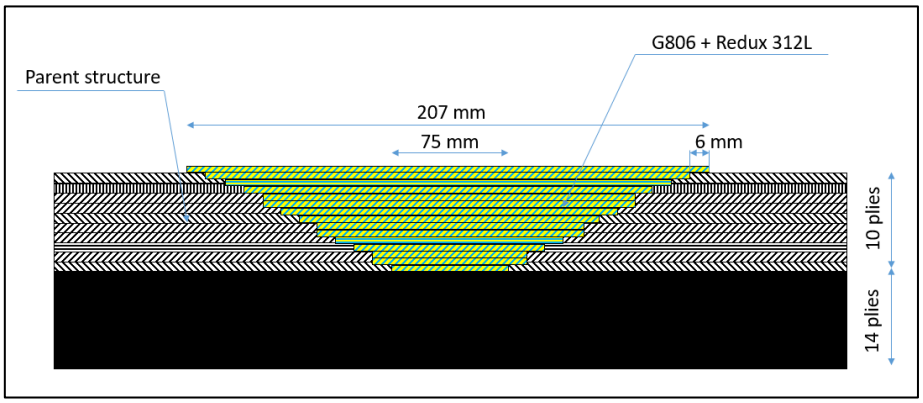

Figure 2 : Flush repair with step machining and wet lay up (WLU) (not to scale)

The second repair is made with an external pre-cured patch, using the same material as the parent composite, but with a modified stacking sequence to achieve a symmetrical layup.

The patches were cured in an autoclave using the same process as the parent material. The hole in the parent structure was filled with paste adhesive, and then the patch was bonded using a film adhesive and a thermal blanket, with the same curing cycle as used for the flush repair (Figure 3). The carrier inside the film adhesive enables a controlled thickness of 0.2 mm along the bond line.

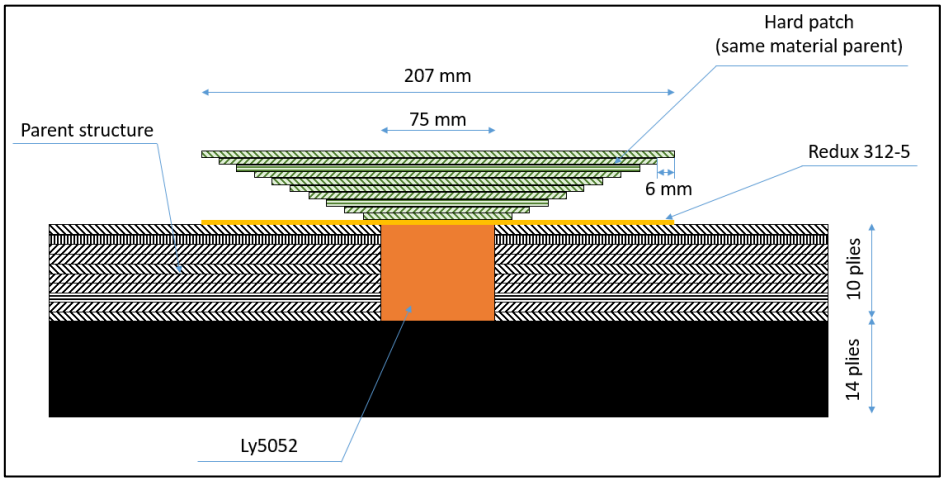

Figure 3 : External repair with a pre-cured patch (not to scale)

The experimental characterization of the two repair strategies was conducted under tensile (Figure 4), compressive (Figure 5), and fatigue loading (Figure 6). Three runs were performed for each type of test and compared to pristine panels.

For the compressive tests, a test device was used to prevent buckling of the panel. The fatigue loading was performed with a R=0.1 ratio to propagate potential damage.

Displacement and strain during static tests were measured by a 3D digital image correlation (DIC) system, strain gauges, and an LVDT sensor. Four acoustic emission sensors were attached to the rear of the specimen to monitor damage evolution. During fatigue tests, acoustic emissions were used to detect three high-amplitude events, to stop the test and perform a lock-in thermography (LT) analysis with a CEDIP Jade LW camera to detect damage initiation in the repair panel.

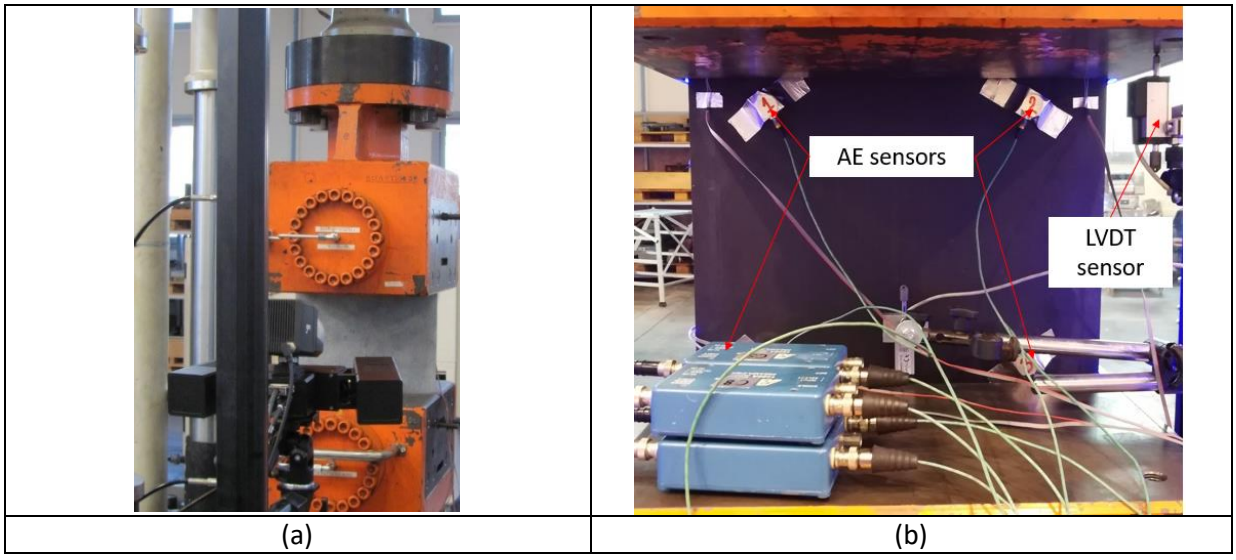

Figure 4 : Experimental set up for tensile tests. (a) Front size (face with the repair) with DIC measurements and (b) AE sensors on the rear side.

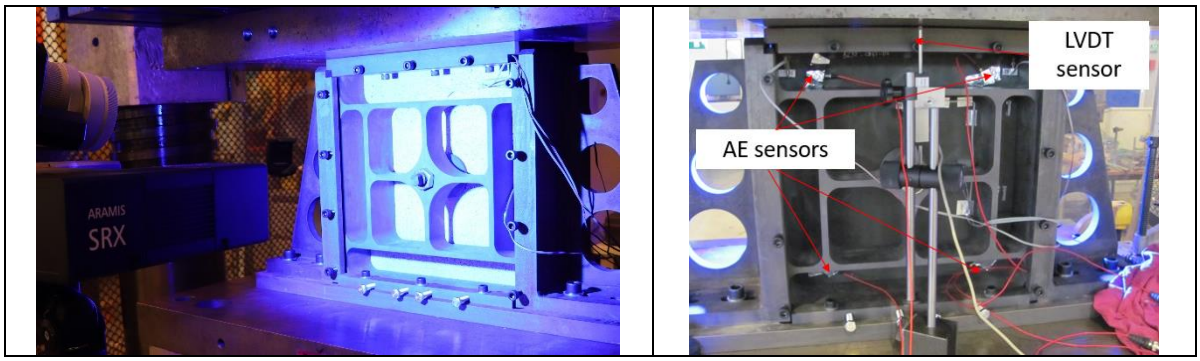

Figure 5 : Experimental set up for compressive tests

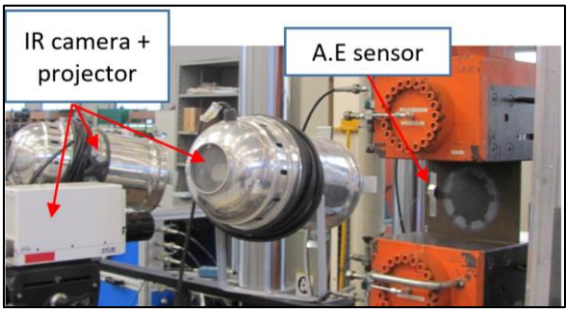

Figure 6 : Experimental set up for fatigue tests

2.1.3. Results

For both repair strategies, the strength recovery compared to the pristine state is almost the same (Figure 7). Although the dry fabric has relatively low mechanical properties (strength and stiffness), the flush repair offers the highest strength recovery at 87%, with a small loss of stiffness (-2%) in tension and almost the same strength recovery (99%) and stiffness loss (-6%) in compression.

The external patch repair shows the lowest strength recovery in tension but increases the stiffness of the panel (+6%), which could be detrimental in a real composite structure, as it may change the load path and create a stress concentration around the repair.

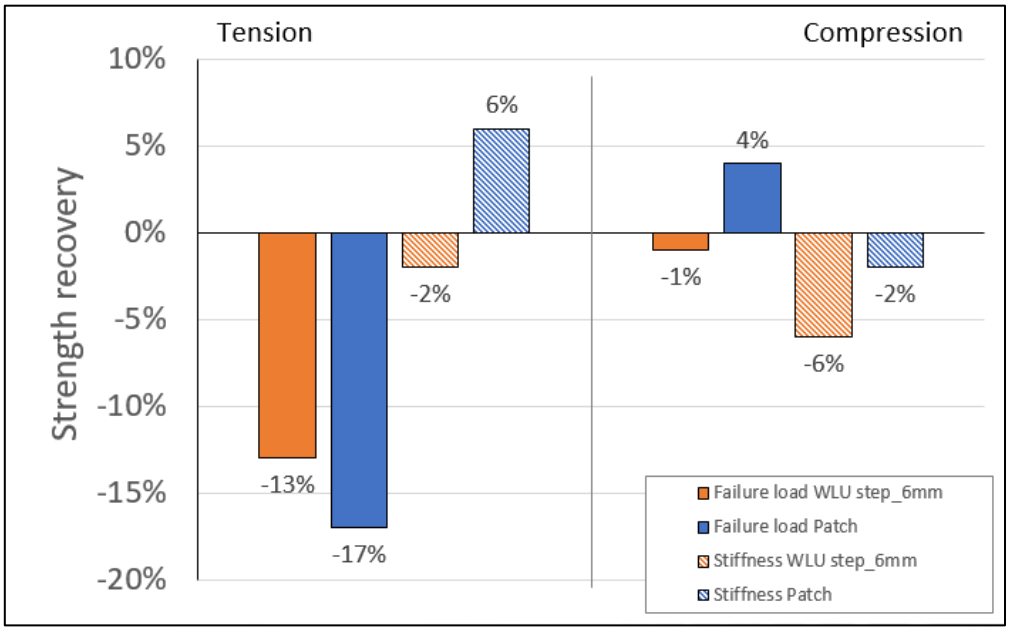

Figure 7 : Mechanical results obtained for both repair strategies compared to pristine panel

The acoustic events (AE) recorded during test show damage initiation starts very early in the panel repaired with the external patch (about 30% of the failure load for both tensile and compressive loading in Figure 8 and 9). For the flush repair, damage begins to appear at approximately 60% and 76% of the failure load in tension and compression, respectively, and increases rapidly until failure.

The pristine panel, on the other hand, exhibits a more continuous damage evolution after damage initiation for both static cases.

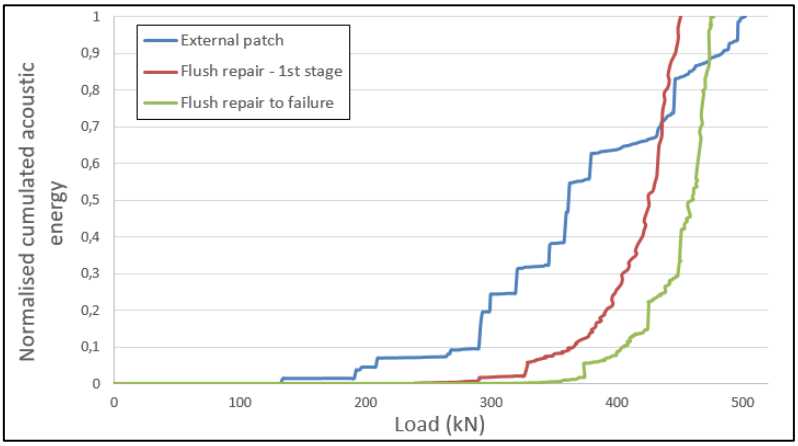

Figure 8 : Normalised cumulated acoustic emission absolute energy of the two types of repaired panels

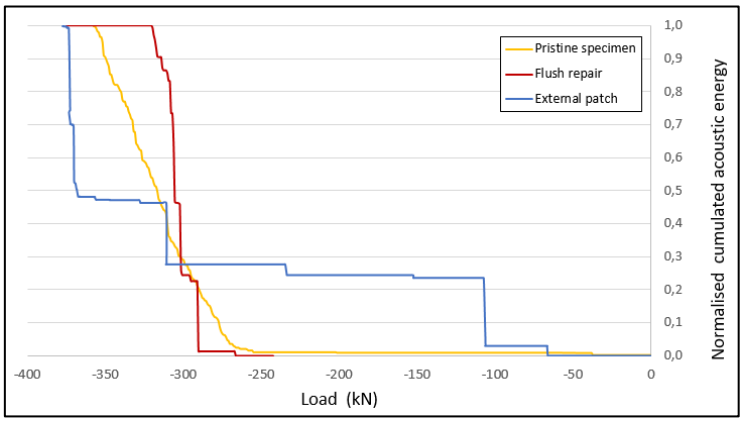

Figure 9 : Normalised cumulated acoustic emission absolute energy of the two types of repaired panels

The flush repair can withstand 40% of the failure load without any damage detected for 5.10^5 cycles, whereas the load has to be reduced at 20% for the external patch to complete 5.10^5 cycles without damage (Figure 10). The fatigue behaviour is consistent with static results since damage initiation occurs at very low stress for the external patch repair leading to rapid damage propagation and panel failure.

	Fatigue life > 5.10^5 cycles without debonding	
Pristine	60 %	Of tensile failure strength of pristine panel
Flush WLU repair	40%	
External patch repair	20%	

Figure 10 : Fatigue results

2.1.4. Conclusion

Two types of repairs were investigated on 4.5 mm thick carbon epoxy panels under static and fatigue loading. A pre-cured external patch made of the same material as the parent was compared to a flush repair, which involved 6 mm steps and a wet lay-up of dry fabric and film adhesive.

Both tensile and compressive results show slightly better mechanical performance (strength and stiffness) for the flush repair, but the acoustic emission (AE) data revealed significant differences in damage initiation and propagation between the two configurations. In the external patch repair, damage initiation occurs at very low loads, followed by slow damage evolution.

These findings are consistent with fatigue results, which showed that even low fatigue loads lead to failure of the external patch repair.

2.2. Methodology for predicting the performance of bonded structural composite repairs in aeronautics.

Contact: ORSATELLI Jean-Baptiste (DGA TA)

2.2.1. Introduction

Bonding assembly offers great potential for the repair of composite structures compared to mechanical assembly using bolts or rivets. Indeed, bonding eliminates the need to drill holes in the structure to be repaired and limits the added mass. However, there is no standard for predicting the strength of bonded repairs, which remain today limited to non-structural applications. This thesis work contributes to the understanding of the sizing of bonded composite repairs, with the main objective of proposing a sizing approach whose cost of use is compatible with use in a design office.

Scientific literature shows that numerous sizing models have been proposed, with a recent trend towards using cohesive zone models for the adhesive and progressive damage models for the composites. The issue of sizing by the "equivalent" joint to the repair is under discussion as a simplified approach to replace complete models.

The proposed approach consists of a double pyramid of modeling and experimental tests to study the representativeness of different scales of bonded repair studies, including the equivalent joint scale and the scale of a complete panel. It relies on material characterization test campaigns. A dialogue between tests and modeling at different scales is proposed to (i) analyze the representativeness of simplified models compared to advanced models, (ii) study the representativeness of small-scale tests compared to specimens at the scale of a complete panel and (iii) discuss the fidelity of models to experimental data.

The case study chosen for this study is that of a co-bonded repair on a Tiger helicopter structure, which connects this study to the industrial context. The materials and processes used in the experimental part are therefore representative of a repair of this type carried out in situ, both for characterization tests and for technological tests.

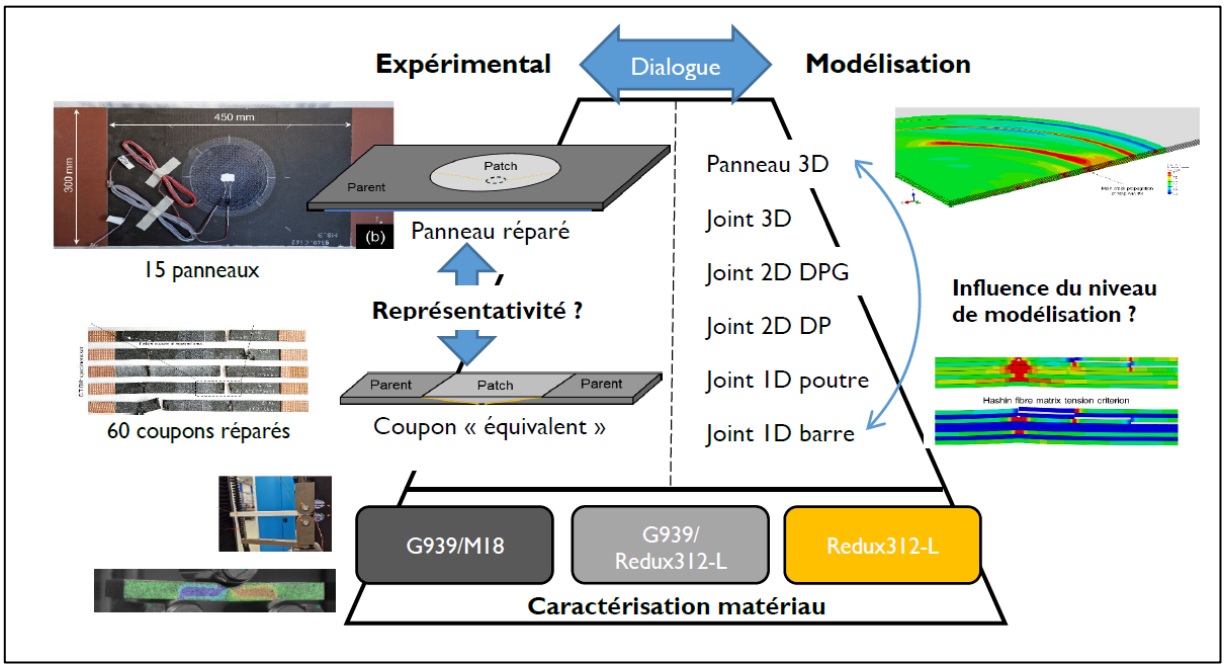

Figure 1: Proposed pyramidal approach.

2.2.2. Work achieved

The characterization tests carried out constitute the basis of the pyramid of the proposed approach. They are divided into two test campaigns. The first focuses on the characterization of the intralaminar and interlaminar behavior of the material of the structure to be repaired, G939/M18, and the repair material, G939/Hexbond 312-L. The second focuses on the characterization of the behavior of Hexbond 312-L as an adhesive in a confined state.

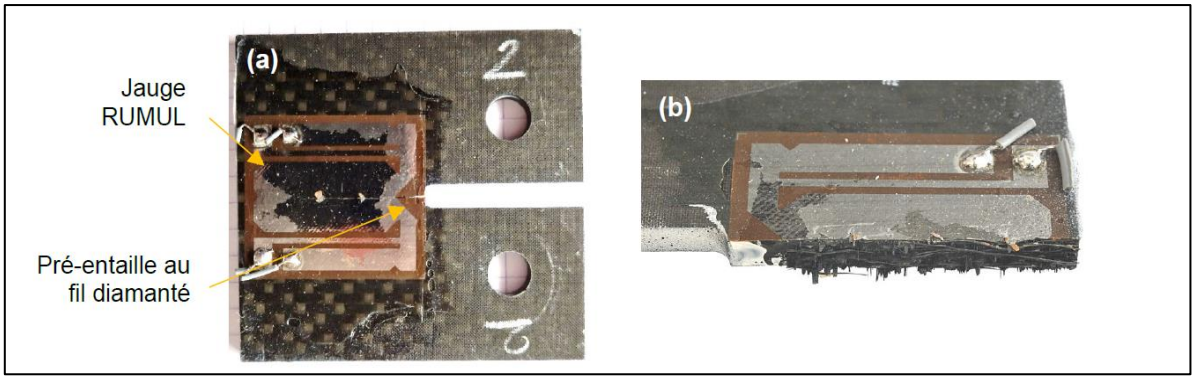

Figure 2: CT tests on composite specimen with RUMUL gauges. (a) Overall appearance after test, (b) view of broken wires after complete rupture of the specimen.

Based on the established set of material property reference data, a comparative study of different modeling scales of a stepping repair was carried out. It contributes to the understanding of the representativeness of low-cost models compared to complete models, and to the development of simplified, robust and fast models for the sizing of repairs. Six different EF and ME models of a repaired panel and its equivalent joint were compared. Ranges of step lengths and adhesive toughness were tested to study configuration variations with respect to the reference configuration.

This study was conducted in a decoupled manner, that is, by first studying the fracture behavior of the adhesive independently of the damage to the substrates. It was shown that the generalized plane strain modeling of the equivalent joint to a repaired panel gives a very good approximation of the stress state in the most loaded section of the repair, as well as the rupture scenario and maximum transfer of the repair.

The 1D bar and beam models are conservative with respect to the repaired panel model outside a range of parameters that groups very brittle adhesives and very short steps. These conclusions were extended to the case where the rupture of the laminates is taken into account.

Finally, the limitations of the proposed models were highlighted by showing that they do not account for any coupling between the patch detachment and the substrate rupture.

For a given modeling level, the associated solution method is also a lever for reducing computation time. Thus, a low-cost stepping repair model was developed from the local equilibrium of a simple overlap joint associated with a nonlinear adhesive behavior of the bilinear traction-separation type.

A semi-analytical solution method was proposed to provide the literature with a new tool for solving this type of problem. It is based on a solution algorithm that searches for the transition points between the linear and damaged domains of the adhesive.

This method was validated by comparing the calculated stress distributions with the results obtained by Macro-Element and Finite-Element resolution.

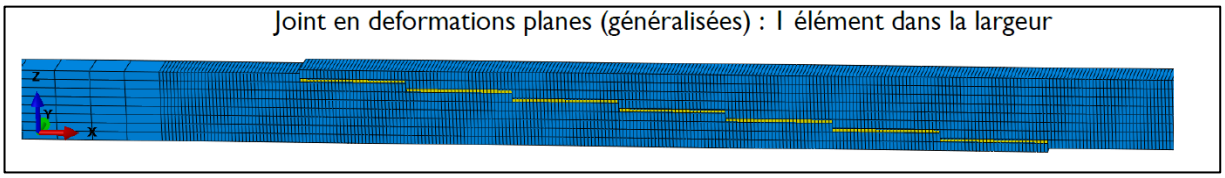

Figure 3: Generalized Plane Strain (GPS) Model

However, it remains limited by the fact that the calculation of the breaking force cannot be done directly due to the instability of the structure at the time of rupture. Knowing this, an approach based on the evaluation of the solution convergence criterion was proposed to give a lower bound of the final breaking force.

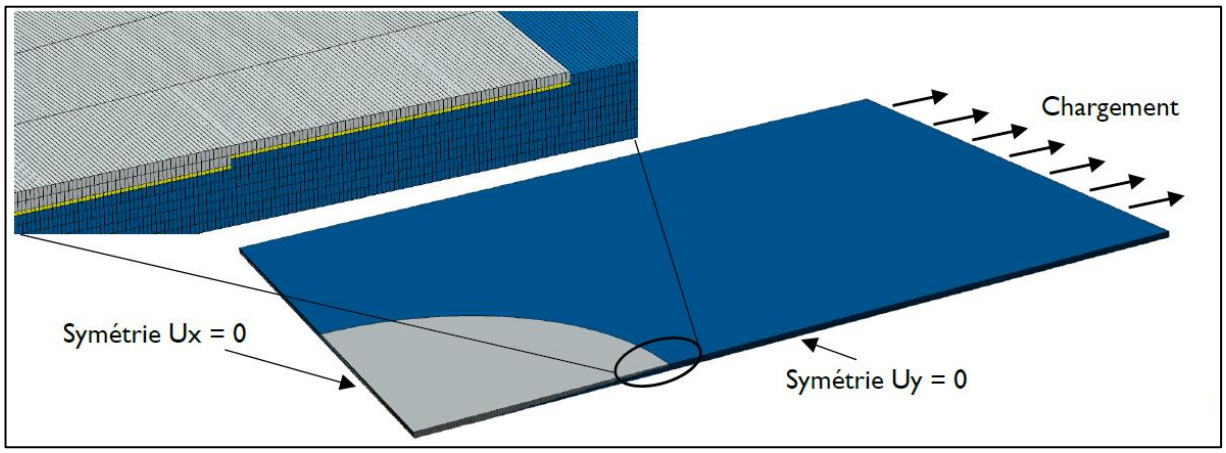

Figure 4: 3D Finite element model.

The multi-scale dialogue approach initiated on the modeling aspect was complemented by an experimental aspect. A test matrix was proposed with the following parameters: step length, damage depth, patch draping and specimen scale. The specimens were manufactured using processes representative of an in-situ repair, including the use of a mobile repair kit. Two types of fracture surfaces were observed depending on the step length: clean laminate rupture for steps of 8 and 12 mm and mixed rupture with delamination for steps of 4 mm.

The step edges appear to be the weak points of this type of repair. The load flow at rupture of the repaired panels is close to that of their equivalent coupons when the step length is sufficient to be outside the transition zone between delamination rupture and laminate rupture. Coupon-scale tests provide a good approximation of the admissible transfer by the repaired panels, and are conservative when the steps are short.

A non-conventional patch draping, of the matching type with a 0° overlap ply, was tested and resulted in an average tensile strength equal to 99% of the tensile

strength of the original material. This result encourages the exploration of innovative patch draping.

A dialogue between experiments and calculations was proposed based on data from technological tests and previously studied modeling.

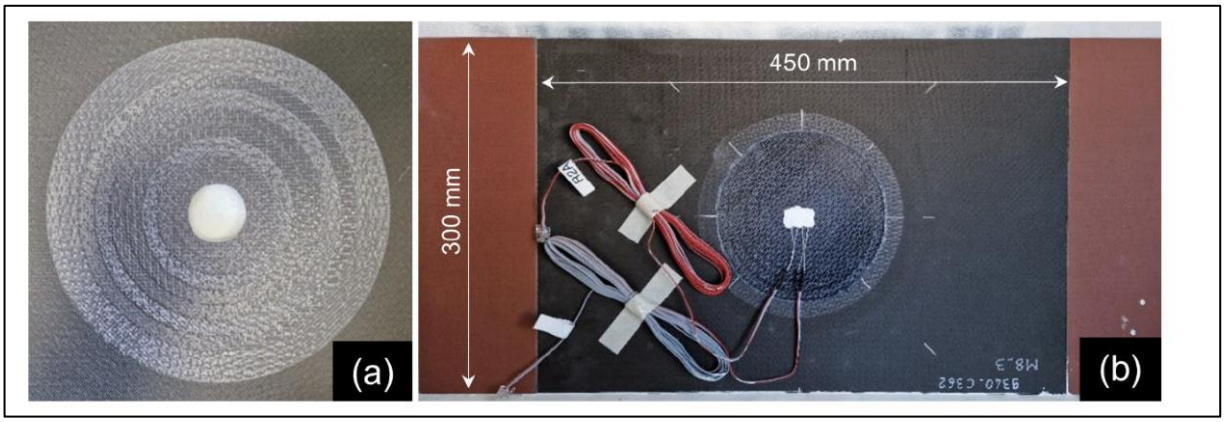

Figure 5: Manufacturing of technological specimens with glued stepping repair.

The EF 2D GPS and 3D models, powered by properties derived from characterization tests, provide results consistent with tests in terms of stiffness and breaking force. The damage scenarios are compatible with experimental observations in most cases. However, tests on 4 mm long step through coupons highlight the limitations of the proposed models, which underestimate the breaking force and do not result in a mixed fracture face as observed.

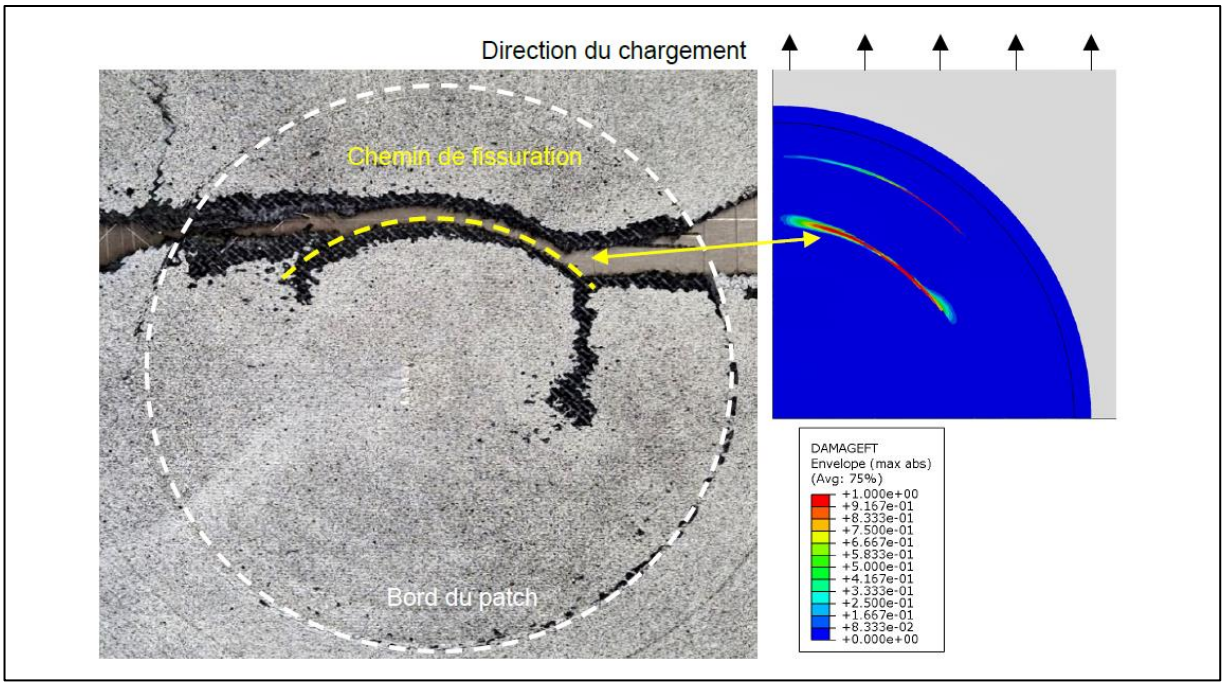

Figure 6: Dialogue experiments-calculations with technological specimens.

Furthermore, the data collected from the tests do not allow to confirm the validity of the damage kinetics of the EF models. Interrupted and multi-instrumented tests should be considered to go further in the dialogue between tests and calculations.

Finally, a parametric script allowing for the automatic generation of EF GPS repair models in stepping was developed. It was used to apply the GPS approach to an industrial repair case involving materials different from the main application case of this thesis, as well as higher skin thicknesses.

The results obtained demonstrate a certain robustness of the proposed approach, which gives results consistent with stiffness and breaking force tests.

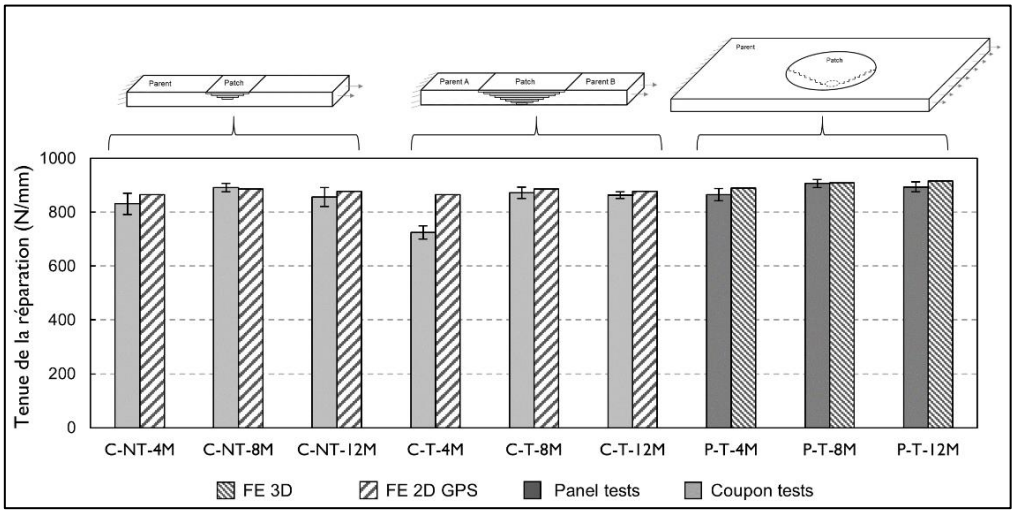

Figure 7: Tests and simulation results comparison.

However, the rupture face seen experimentally, involving delamination under the patch, is not found in FE simulation.

The developed script was also used to propose a stepping repair optimization strategy. Unlike the reference method which determines overlap lengths only from the surface ply orientations at the stepping level, the proposed method takes into account the behavior of the entire repair via a 2D GPS EF model to optimize the different step lengths. Numerical tests were carried out, showing that the proposed method correctly retrieves the logic of the reference method, which assigns a maximum step length at the level of the 0° ply.

It results in a theoretical encumbrance gain greater than the reference method, with constant theoretical hold, by further reducing the overlap lengths at the level of the 45° ply. This approach would need to be validated by experimental tests to evaluate the strength of the optimized configurations obtained.

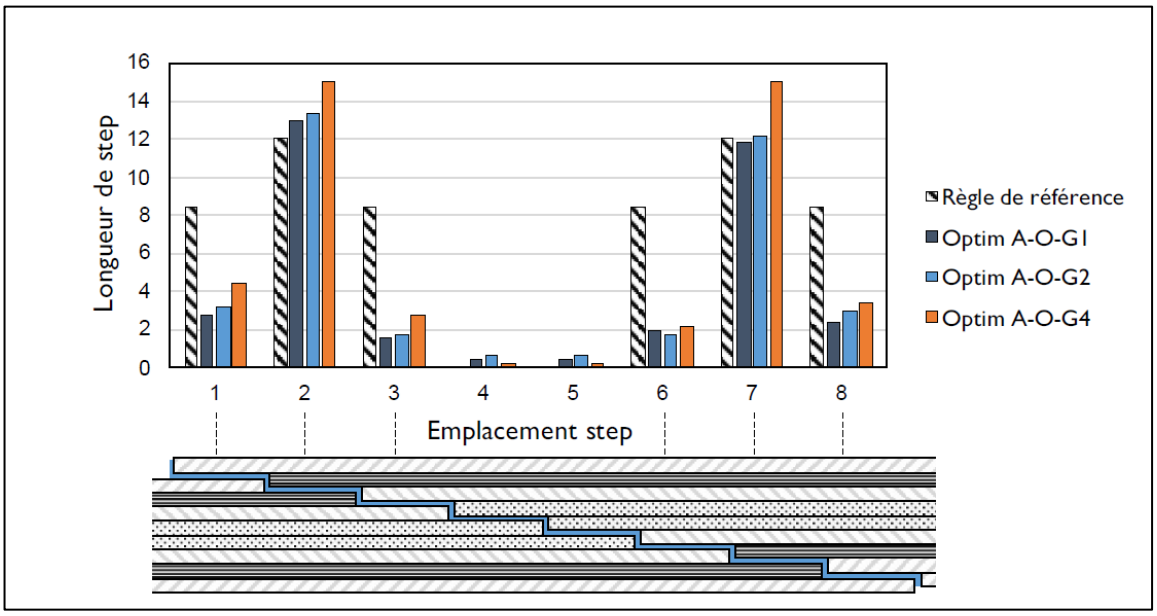

Figure 7: Optimization of stepping lengths via the reference rule and the developed algorithm.

2.2.3. Perspectives

The models developed in this work and their validation based on experimental results are part of a process to develop virtual testing tools for the design of composite repairs. Further work could be considered to increase the level of confidence in the sizing models, and to move towards an approach compatible with certification requirements in terms of aircraft airworthiness.

In addition to mastering the characterization of material behavior, a study of the sensitivity of the models to variations in input properties can be proposed. This would allow conclusions to be drawn about the robustness of the models in the event of errors or variability in the properties of the materials involved. The difficulty of this type of sensitivity study is to control the number of calculations to be performed given the number of material properties involved, even with simple damage models.

The technological tests proposed in these works did not allow for a discussion of the damage kinetics determined by the EF models. To the author's knowledge, there are few or no studies on bonded composite repairs that have provided experimental data to validate a complete damage scenario.

Conducting multi-instrumented tests, for example with acoustic emission (AE) and infrared thermography (IR) measurements, or interrupted tests, is a research

track to go further in this discussion, but these approaches remain complex to implement. Moreover, the question of the coupling between substrate debonding and laminate rupture needs to be studied in order to propose a design logic for bonded composite repairs.

However, the materials and step lengths involved in the mentioned study do not allow for a configuration with a clean laminate rupture as would be sought for a structural repair, and therefore to observe the transition between debonding rupture, delamination rupture and fiber rupture.

Research on load cases other than uniaxial tension is an avenue to be pursued. Indeed, uniaxial tension remains today the most studied load case in the scientific literature. Compression, bending, and biaxial loading can be mentioned among other cases to be studied. Beyond the validation of complete models, the question of the representativeness of a typical joint equivalent model in GPS in these load cases is an axis to explore to extend the conclusions of these works.

Moreover, the question of the durability of repairs is also an important issue. The design of a bonded composite repair that stands the test of time involves several aspects, including aging in a humid atmosphere, fatigue resistance or compressive strength after impact. These different aspects are to be addressed from both an experimental and a modeling point of view.

The use of simplified geometry models of the GPS type as studied in these works can constitute a research axis to address these complex sizing cases at a lower cost.

Beyond the lock of the sizing of a bonded composite repair, the question of mastering the manufacturing processes remains to be studied to achieve certifiable repairs. Indeed, even if non-destructive testing (NDT) methods can be used to control the quality of a bonded assembly, it is still difficult today to ensure its strength on the basis of an NDT. In particular, ultrasonic testing methods can detect porosities or air gaps in bonded joints, but can hardly detect kiss bonding type defects, that is, weak adhesion between the substrate and the patch.

The development of process control approaches can be considered to attest to the quality and reproducibility of the production of a bonded assembly. To do this, quality control by a supervision-simulation approach can be considered, as proposed in the collaborative project S3PAC[1] (system for supervision and simulation of the production of bonded assemblies). The automation of the machining of repairs, for example using robots such as the REPLY5 marketed by BAYAB Industries, constitutes

a first step forward in terms of reproducibility of the repair process, compared to manual machining.

Finally, the integration of manufacturing process monitoring sensors, or Process Health Monitoring, could also allow monitoring of the polymerization cycles of repairs to provide data to control the quality of the processes implemented, provided that their non-intrusive nature is demonstrated. Bragg grating fibers or QRS® sensors marketed by SENSE in ® are examples of such sensors. They can also be applied to Structural Health Monitoring of structures during their operational life, to address the issue of monitoring the long-term performance of bonded composite repairs.

[1] Agathe Jaillon, Thèse de doctorat, « Étude expérimentale et numérique du comportement à rupture des assemblages collés à épaisseur de couche adhésive variable ». ISAE-SUPAERO, Toulouse, 2020.

3. Full-scale fatigue testing

3.1. Supplementary fatigue substantiation work on aircraft elements required for the extension of the service life of the aircraft cells (outside the scope of the Fatigue Test Cell).

Contact: M POMMEPUY Nicolas (DGA TA)

3.1.1. Context.

Further work is needed to justify the extension of service life for main components common to and/or specific to the different versions of the aircraft. These elements are not present on the CEF because it is not possible to carry out their loading directly onto the CEF.

3.1.2. Objective and description of the tests to be carried out by DGA TA

The specimens involved in these tests include, among others, the traps of the front landing gear and the main landing gear. These tests use carbon composite, NIDA as well as metallic parts.

The objective of these tests is to validate a service life for the front trap fittings similar to that of the rest of the aircraft structure. This service life will be initially determined from a safety factor identical to that of most other parts and then with a higher safety factor.

Finally, depending on the condition of the specimen at the end of the fatigue tests, residual strength tests up to ultimate load will be carried out.

The spectra applied to these parts take into account the stresses generated during all flight phases for all planned missions: takeoffs/landings, catapults/arrests, Touch And Go (TAG), ground maneuvers, etc.

Views of the test setup are presented in the Figure 1, hereafter:

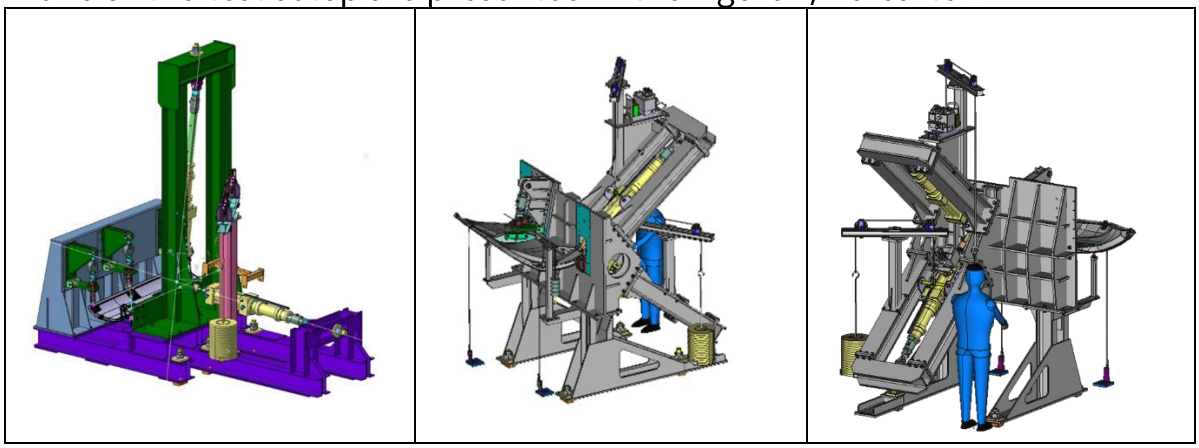

Figure 1: Trap landing gear set up.

3.2. Description of fatigue tests for NARANG aerial refuelling pod

Contacts: FRAISSE François-Xavier (Safran Aerosystem), TORRELLI Raphaël (DGA TA), OULD HAMMOU Yamina. (DGA TA)

3.2.1. Presentation of the test.

The objective of this fatigue test is to realize the qualification, for quasi-static fatigue loading, of the New Generation Aerial Refueling Pod (NARANG stands for NAcelle de RAvitaillement Nouvelle Generation) which equips the French Navy's RAFALE fighter aircraft. A photography of the aerial refueling pod NARANG is presented in the Figure 1 below:

Figure 1: NARANG aerial refueling pod

For that purpose, the test has to validate the fatigue life of the structure with a safety factor. Below in Figure 2, is a part of the nacelle in its test facility:

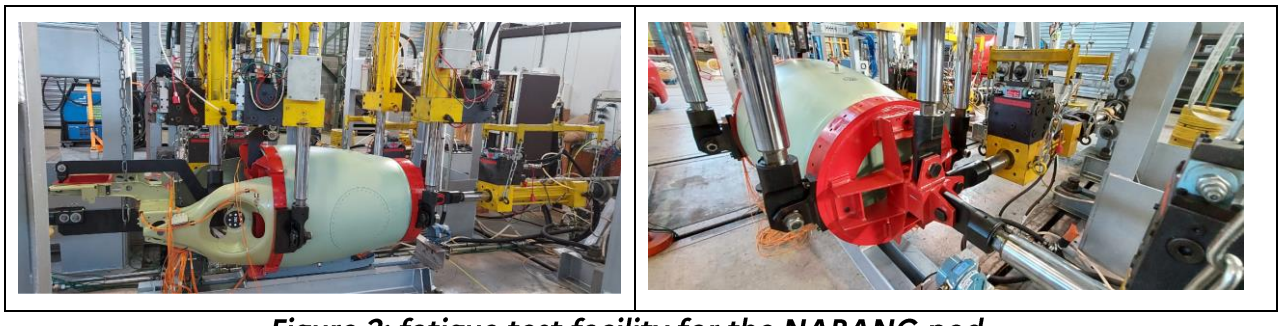

Figure 2: fatigue test facility for the NARANG pod

Quasi-static fatigue loading is introduced using 12 hydraulic jacks. The Figure 3 below shows the position of the hydraulic jacks:

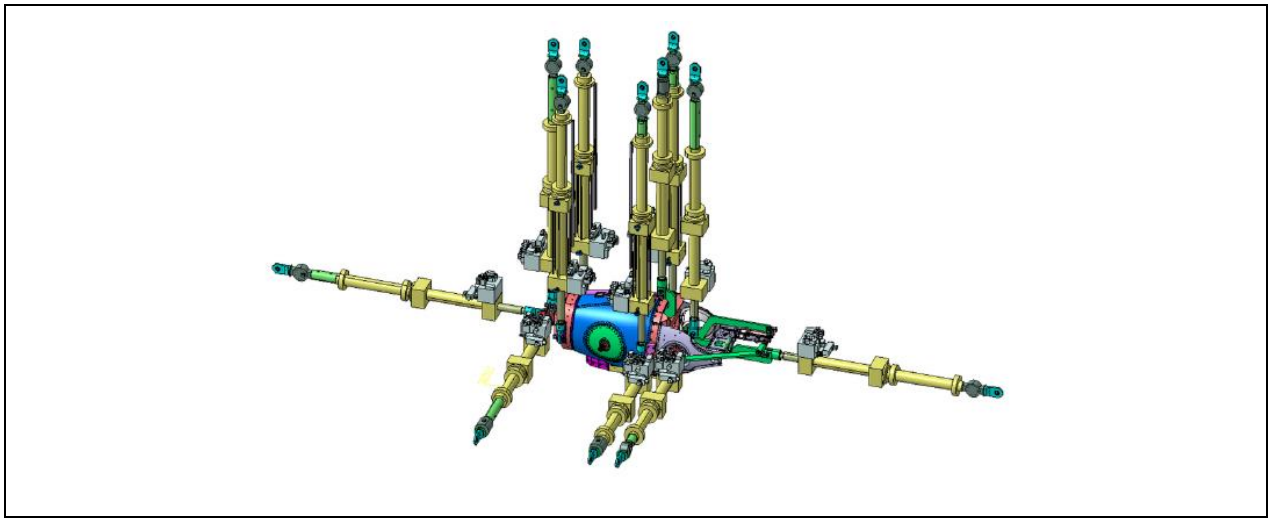

Figure 3: Hydraulic jacks set up

3.2.2. Presentation of the test instrumentation.

Moreover, as shown in the Figure 4 below, four pressure measurement stitches and one inflation tip are used to ensure the fuel pressurization of the nacelle during the test.

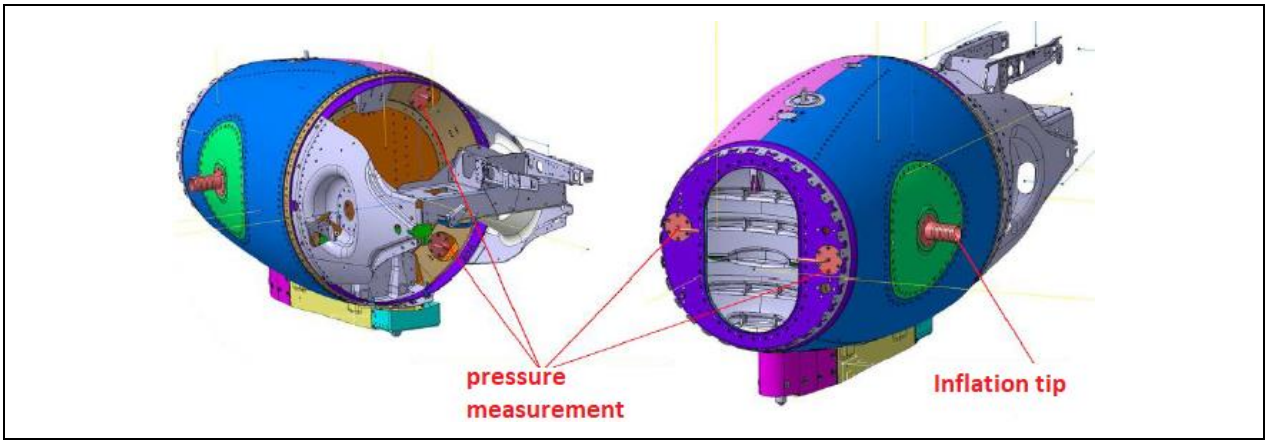

Figure 4: pressure measurement stitches and one inflation tip position

The nacelle is equipped with strain gauges and displacement sensors and NDT checks are carried out at regular intervals during the test to detect any damage.

To guarantee the integrity of boundary conditions during a fatigue test is a major issue. During the test, it is necessary to check the tensile preload of certain bolts.

3.2.3. Verification of the preload

The sole is a critical part in the test, it is placed at the boundary of the NARANG and used to represent the interface with the aircraft (pylon). Four bolts are used to fix the sole to the NARANG. The aim of these bolts is to link these parts by introducing a restoring force called "preload" force.

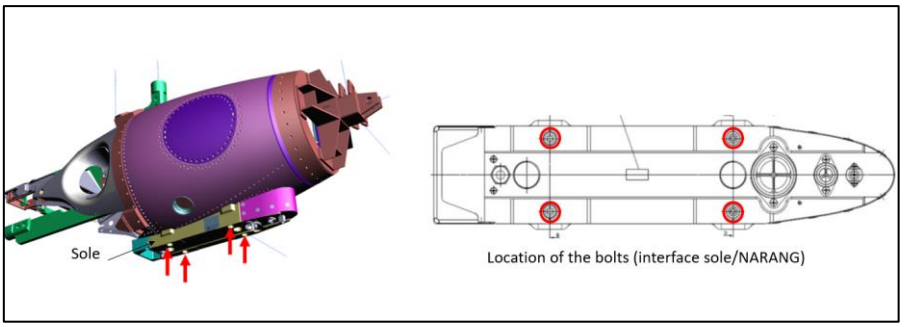

Figure 5: Position of the 4 bolts preloaded

An usual way to tight bolts is to use tools based on torque measurement (for example: torque wrench). Because most of the applied torque is converted into friction forces (in threads, under bolt head…) ensuring that the required preload force has been correctly installed could be challenging. To overcome this issue, an innovative device based on ultra-sonic wave has been used.

The principle is to introduce a high frequency (20 MHz) ultra-sonic pulse into the bolt and measure the delay T to receive the wave reflected by the bolt's opposite edge (see Figure 6). This delay is converted to a length.

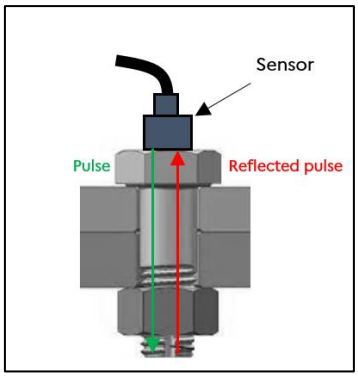

Figure 6: Ultra-Sound pulse path in the bolt.

The pre-load force F_O in the bolt is then computed from the variation of length (elongation) ΔL of the bolt before and after the tightening (see Figure 7).

The effect of the temperature is also took into account within the measurement process.

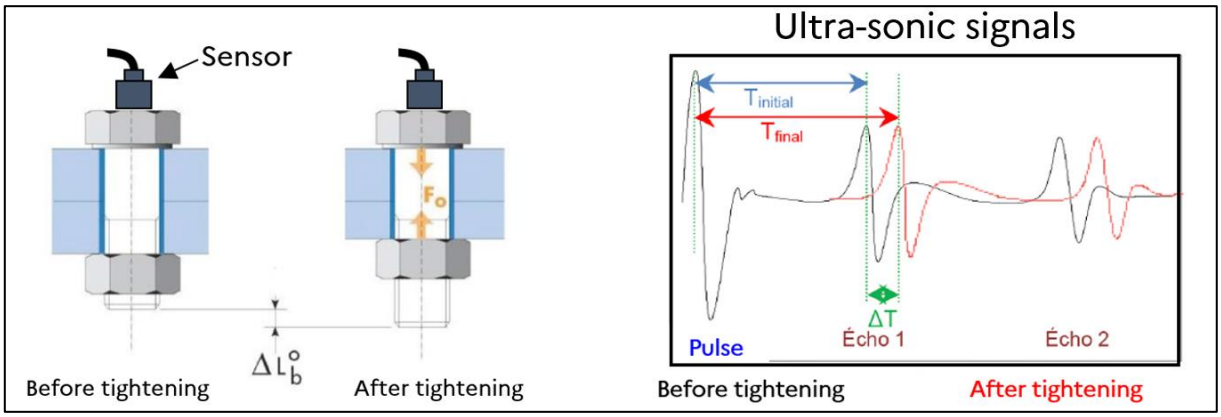

Figure 7: Preload force measurement by US pulse delay.

The ultra-sonic measurement is a non-intrusive method, easy and fast to handle. On the NARANG fatigue test, this technique is used to monitor the pre-load on a critical interface.

3.3. Improvement of knowledge in control, corrosion and mechanical behavior of ATL2 structures: ACCROCS (Amélioration des Connaissances en Contrôle, corROsion and comportement méCanique des Structures d'ATL2).

Contact: GUIGUE Alexandre (DGA TA)

3.3.1. Context.

Atlantique 2 (Figure 1) is an aircraft operated by the French Aeronaval forces. Its uniqueness resides in its outer wings composition: an aluminium material sandwich. If this material provides a good bending stiffness over weight ratio, corrosion has been found between the skin and the core (disbonding) of this material close to wings ribs and spars. French maintenance workshops, in collaboration with DGA TA, issued a maintenance schedule in order to anticipate debonding, to track and repair the potential defaults on the fleet.

Figure 1: ATL2 in flight

DGA TA, a large-scale structure-testing centre, suggested further testing from an entire wing. The objectives consist in a better knowledge of debonding propagation on a three-dimension structure and the behavior of innovative repair solutions on a large scale on an internal methodology test while inputting a global scale load.

This enables DGA TA to maintain its knowledge in full-scale testing, mixing instrumentation such as large window Digital Image Correlation (DIC), strain gauges, Fiber Bragg Grating and large displacement camera measurements.

The test specimen used by DGA TA is a half extreme wing of the Atlantic 2 M10, about twelve meters long. This specimen was recovered following the decommissioning of this aircraft.

Figure 1: Test installation in hall 6 and specimen.

3.3.2. Description of the test setup and loading.

This project involved numerous departments of DGA TA and solicited many internal expertise: structural calculation, test design, assembly, preparation of active systems, piloting, measurement acquisition, metrology and non-destructive testing.

In preparation for the test, the Structures Tests and Expertise department conducted a finite element numerical calculation aiming to predict the deformations and displacements of the specimen, which allowed the design office to design the test installation. The extreme half-wing is taken back to the wall through a specific frame designed by the DGA TA design office.

Three carcans distribute the bending effort upwards and rest on the rigid elements of the wing: the intersections of the longerons with the ribs. These carcans are connected to six vertical effort lines on the extrados of the wing. Three are located at the leading edge and three at the trailing edge. These allow bending and torsion efforts to be introduced into the half-wing.

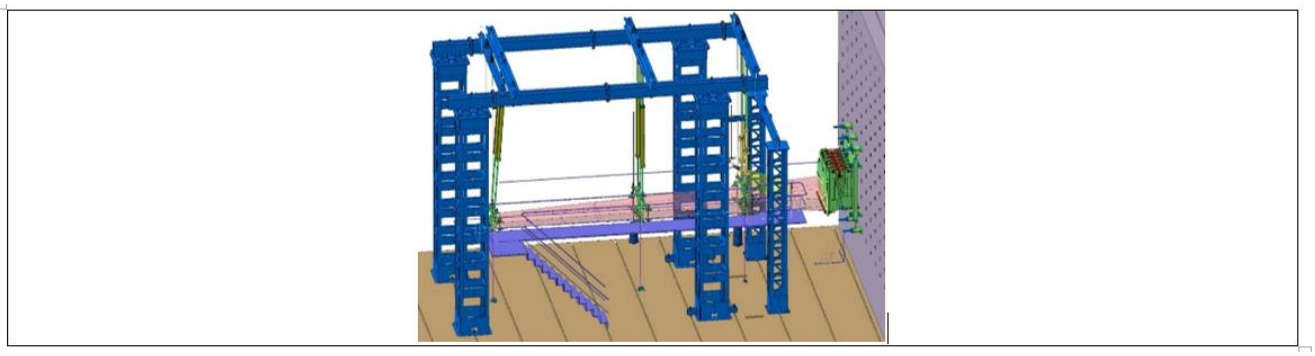

Figure 2: Computer-aided design of the ACCROCS test facility

3.3.3. Description of the test instrumentation.

During this same phase, in collaboration with "ISAE Supaéro" and the Materials and Technologies (MT) Division, skin-to-spar delaminations were introduced on the specimen. Subsequently, repairs as performed on aircraft were implemented by the "Atelier Industriel de l'Aéronautique" (Aeronautical Industrial Workshop) of Cuers, which also prepared an area for the application by DGA TA of a repair by bonded composite patch with the objective of comparing the behavior of these repairs to that of the damaged areas without repair under fatigue loading

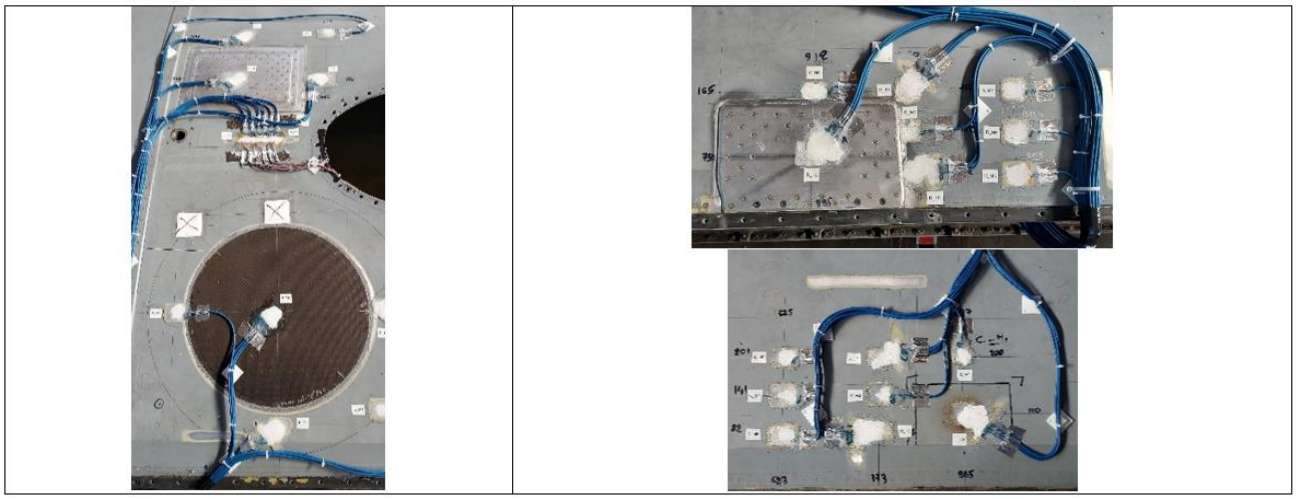

Figure 3: Composite patch, areas repaired by AI and thermally delaminated area.

Once these preparations were completed, the installation was set up in the Test Hall by the Structures Test Implementation Department. Finally, in addition to conventional instrumentation consisting of 78 channels of strain sensors and 8 channels of displacement, the test was an opportunity to install innovative instrumentation with the help of the Engineering Means Division (IM), namely large-field image DIC as well as Bragg gratings (deformation measured with optical fibers).

3.3.4. Description of the DIC installation.

The ACCROCS test phase began with preliminary static unitary cases which allowed validation of the installation: six unitary bending cases and two torsion cases. Once these adjustments were complete, a fatigue spectrum was applied. This spectrum includes six different missions and represents one thousand flight hours for the aircraft. A total of five complete spectra were applied to the specimen from mid-2023 to early 2024.

DIC of "wide field" images made it possible to test the measurement means at the level of the wing's extrados, at the wing-wall interface, where the expected deformations are the most important. Thanks to two cameras filming a surface that is subjected to a mechanical load, stereo-correlation allows the acquisition of the 3D displacement and deformation field of this surface over time. This method works in the same way as a point tracking in images and therefore requires the deposition of a random pattern, called a speckle, on the measurement surface.

One of the challenges to be met in the context of ACCROCS was the deposition of a suitable speckle, with controlled characteristics, in relatively unusual conditions: large measurement area (more than one square meter) and already assembled wing (horizontal surface instead of vertical, without possibility of moving it). For this reason, a new deposition method using a water-soluble film of A4 size was used. This process allows the deposition of a printed pattern, previously defined by the operator.

In the context of ACCROCS, due to the large size of the surface, and in order to open up the perspectives of multi-scale instrumentation, the choice was made for a so-called "fractal" pattern. The mechanical behaviour of the water-soluble film had been previously studied in tension/compression on elementary specimens in a joint IM/MT/ST study.

The ACCROCS pattern presented good metrological properties considering the area of the surface (cf. Figure 5), and followed the deformations of the specimen well, even in the buckled areas at rupture.

Another challenge in terms of camera instrumentation was the production of a measurement at each remarkable level of the fatigue loading cycles, and this synchronously with the test control system.

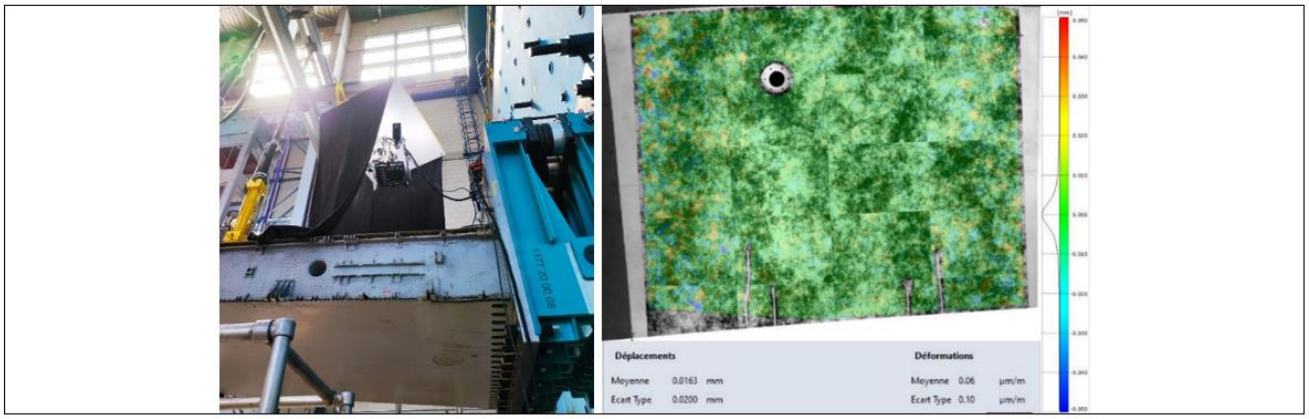

Figure 4: On the left: measurement method by DIC. On the right: measurement of uncertainties on the fractal pattern.

3.3.5. Results and conclusion.

In summary, the ACCROCS test validates the possibility for DGA TA to offer a large-field measurement service over a wide area in the context of future tests with good accuracy.

The peculiarity of the test inherent to the delamination introduced illustrates the interest of this type of measurement: the heterogeneity of the deformation field at the level of the defect introduced at the skin-core interface of the extrados could be captured (cf. Figure 5).

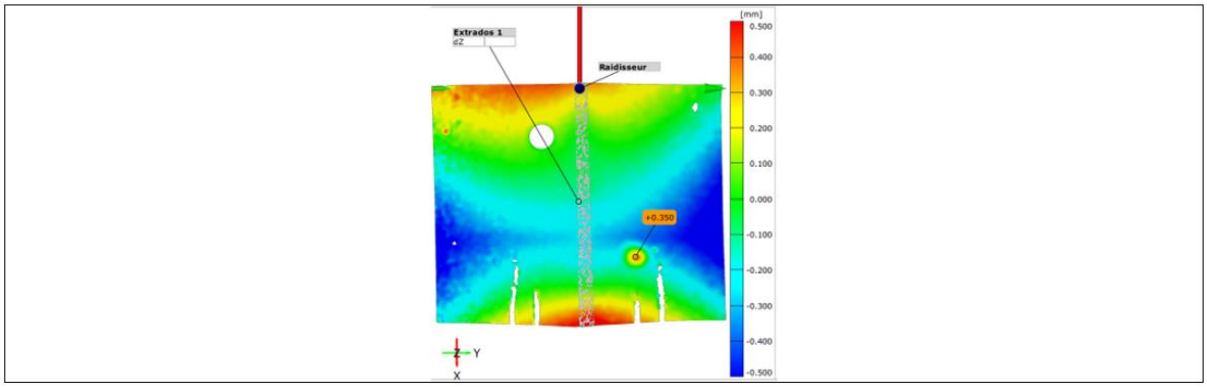

Figure 5: Vertical displacement field by DIC during a specimen bending.

This phase of tests which originally was to be the only one was finally followed by another one in order to prepare the loading and acquisition systems for the future tests within the Structures division of DGA TA which chose to take advantage of the installation in place. This second phase which went up to the specimen's rupture ended at the beginning of 2024.

4. Sustainable aviation

No specific study to present in this chapter.

5. Reliability and risk analysis of structures and mechanism

No specific study to present in this chapter.

6. Advanced materials and innovative structural concepts

No specific study to present in this chapter.

7. Fatigue life enhancement methods and repair solutions

No specific study to present in this chapter.

8. NDI inspections and structural health / loads monitoring

8.1. Comparison of various health monitoring processes of a composite: Infrared Thermography, Acoustic Emission, DIC and Sensity Tech®.

Contacts: Anna Pugach (Touch Sensity) / Mehdi Elhafed (Touch Sensity) / Marc Briant (Touch Sensity) / Sophie Mougeot (DGA TA) / Gregory Lacoste (DGA TA) / Franck Sanz (DGA TA) / Christian Cavailes (DGA TA)

8.1.1. Introduction

As part of SHM technology watch activities, DGA TA has met with the Touch Sensity Start Up several times in recent years.

The TOUCH SENSITY start-up was founded in December 2019 following the development of Sensity Tech® technology. This non-invasive technology makes materials communicative, capable of detecting, tracking and evaluating any mechanical stress as well as damage. It thus offers continuous monitoring of the structural condition of materials throughout their life (during manufacturing and/or operation), contributing to improving their reliability, safety and durability.

Sensity Tech® is presented as follows: "This innovative technology could be applied to carbon composite materials directly connected to the fibers or non-carbon materials through a sensitive coating." The operation of Sensity Tech® is based on the interaction of three elements:

- A material that you want to make sensitive.
- An embedded system connected to the periphery of the material to be monitored, allowing data acquisition.
- A signal processing system allowing to reconstruct in the form of a 2D/3D mapping view the structural state of the material, precisely identifying the modifications and damage suffered as well as nascent or propagating damage, whether internal or superficial.

Sensity Tech® is therefore a complete system for data acquisition and processing, capable of adapting to environmental constraints (humidity, temperature, etc.).

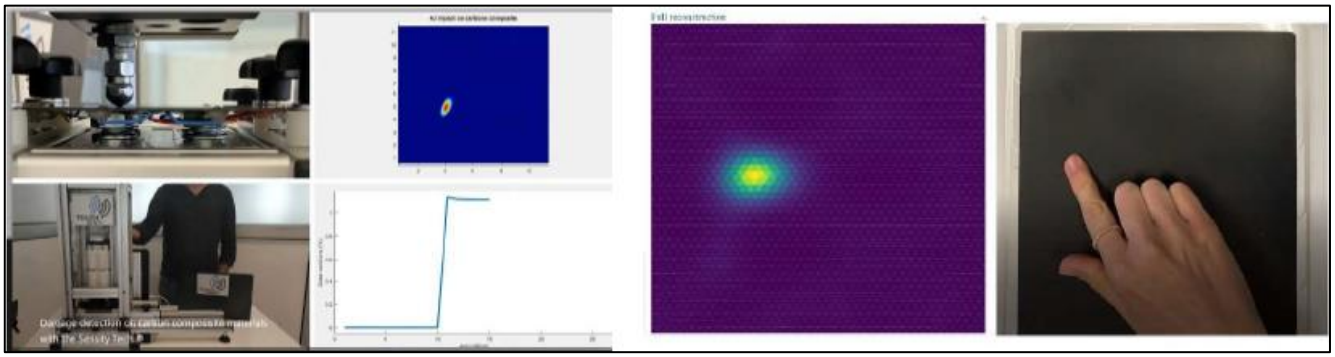

Figure 1: From left to right, illustrations of Sensity Tech® technology applied to carbon fiber composites and sensitive coating.

Several patents have been issued by the company and present a technology that can provide technical SHM solutions for MCO.

8.1.2. Tests objectives

In this context, DGA TA conducted a first standard tensile test. The test aims to evaluate the capabilities of Sensity Tech® technology in the field of monitoring composite materials and is part of a broader approach to validate the effectiveness of SHM technologies for real-time monitoring of the condition of materials, with a view to their application in predictive maintenance and non-destructive testing.

This test aims to :

- Assess the technological maturity level of Sensity Tech®.
- Verify the technology's ability to detect and locate rupture initiation events in a composite material during a tensile test.
- Compare the performance of Sensity Tech® with other monitoring methods to evaluate its ability to detect the early appearance of defects in composites, complement existing data on the technology.
- Provide a better technical understanding of this innovative technology, protected by several patents.
- Evaluate the application potential of Sensity Tech® for real-time monitoring of material condition, with a view to its application in predictive maintenance and non-destructive testing.

8.1.2.1. Specimen identification for testing

Two batches of eight composite test specien were manufactured by DGA TA. The material is carbon/epoxy type: M18-1 / G939 draped in 16 quasi-isotropic plies.

The first batch was used for the preparation phase of the test machine and measurement systems.

On the second batch, the TOUCH SENSITY company prepared the connectors for the 4 samples to be tested. The other 4 samples are used by TOUCH SENSITY company as a reference and calibration for Sensity Tech®. These are returned intact at the end of the service.

Figure 2: The 4 test tubes with connectors

8.1.2.2. Test setup description

Each test specimen held by the grips of the tensile testing machine is monitored by Digital Image Correlation (DIC) systems, acoustic emission and infrared thermography, as shown in the following photograph:

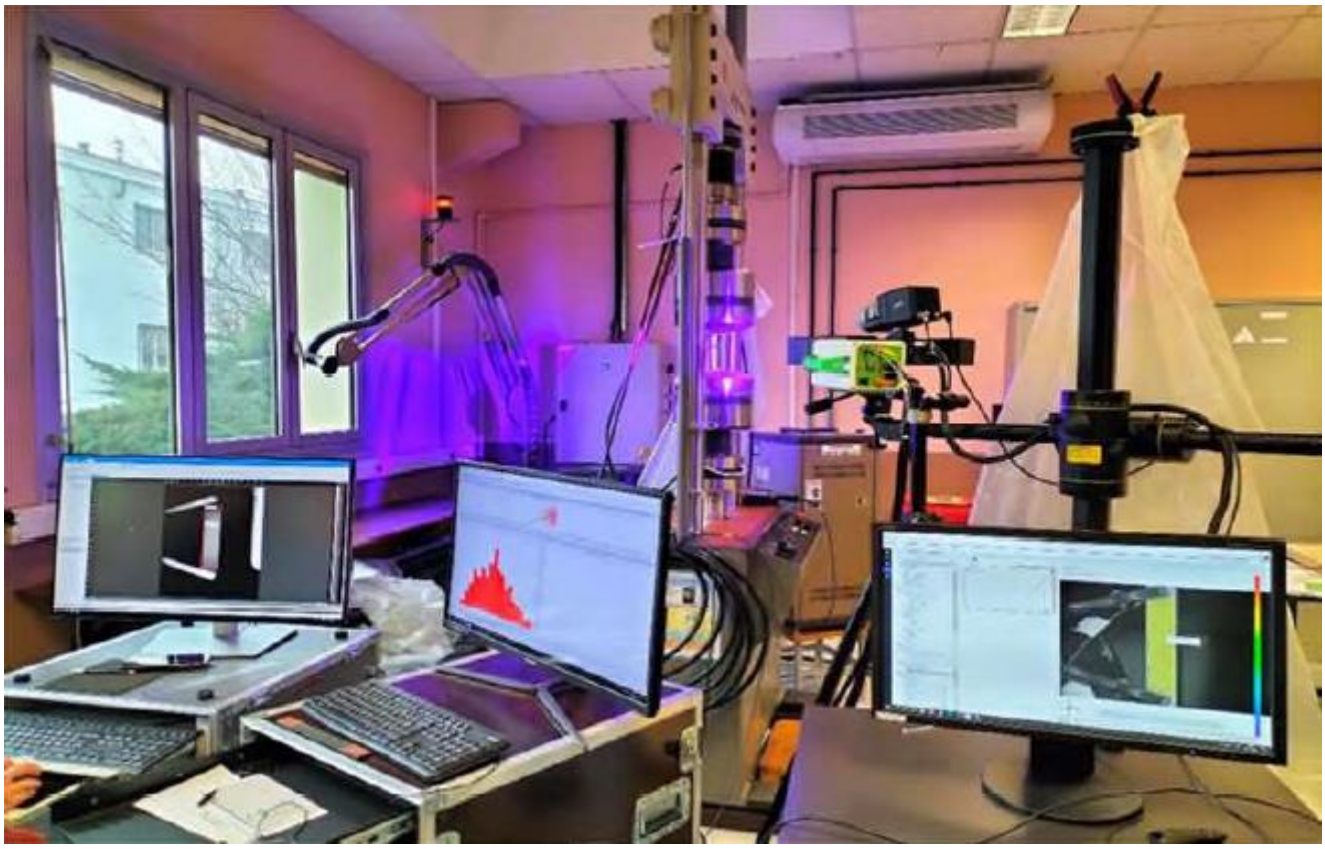

Figure 3: From left to right, the acquisition systems: Infrared Thermography, Acoustic Emission and Digital Image Correlation (DIC)

8.1.2.3. Location of measurements on test specimens

The four test samples are wired to the Sensity Tech® acquisition system; two acoustic sensors are glued to listen to the central area of the test sample.

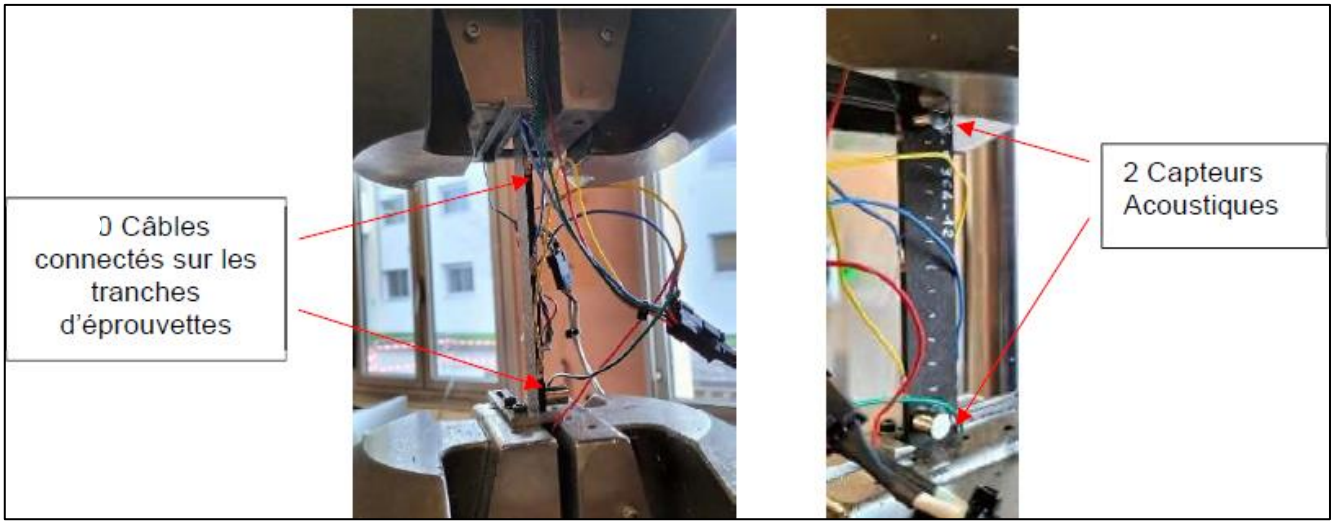

Figure 4: Instrumented composite sample on the testing machine

8.1.2.4. Specific conditions of the test

The test carried out at room temperature includes:

- Phase 1: clamping of the machine jaws and recording of events by Sensity Tech®.

- Phase 2: application of load cycles for 3 specimens and a continuous traction for one specimen.

The cycles were established during the preparation of the tests and allowed to determine a breaking effort close to 60KN. In order to highlight the appearance of internal defects, cycles of uploads and discharges were established from the detection of internal events in the composite material, measured by acoustic emission.

8.1.3. Presentation of the results

8.1.3.1. Test Phase 1: jaws tightening

The raw result curves, obtained with Sensity Tech® technology, presented during the tests with the mappings of the four specimens at the end of tightening, show some dispersion according to the specimens and extremely low internal intensity values, 10 times lower than that of an elongation of 0.1% for a rupture at approximately 2%.

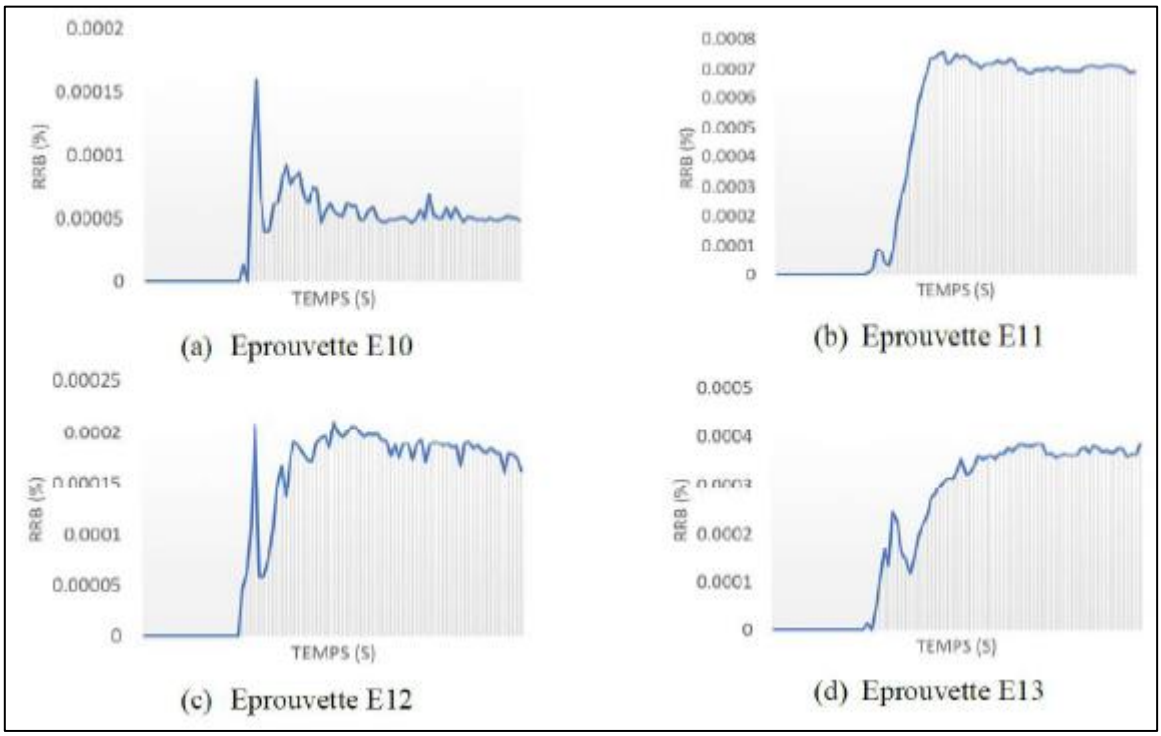

Figure 5: Raw responses calculated by Sensity Tech® during jaw clamping.

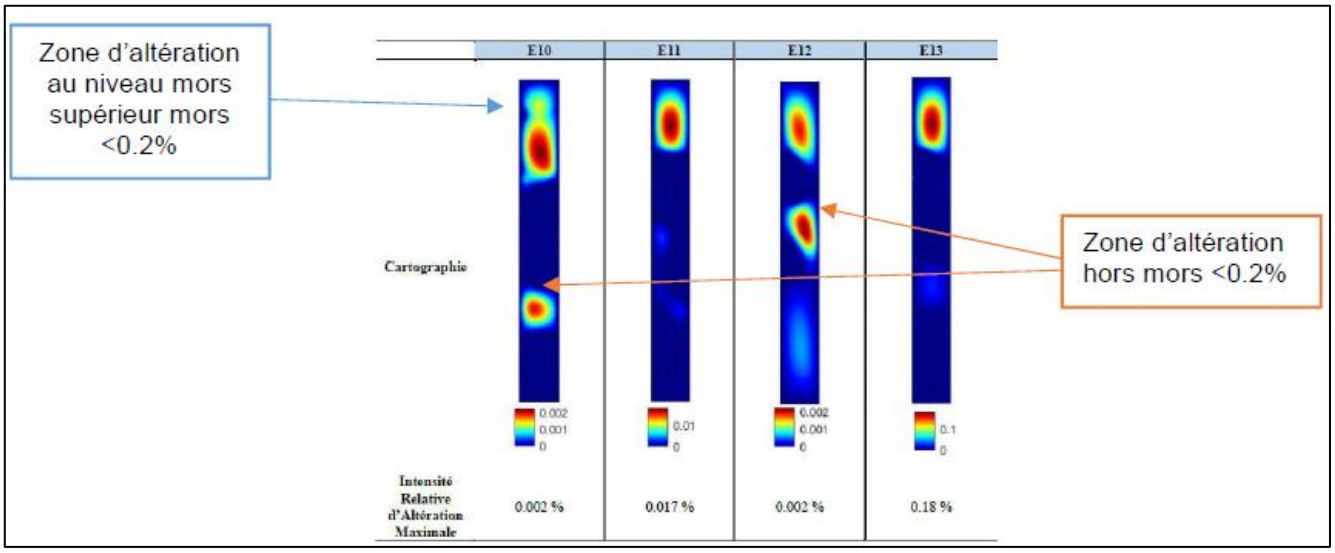

Figure 6: Reconstruction of the internal state by Sensity Tech®

These elements, in addition to DIC, ensure that the specimens have not undergone deformation during placement and that clamping does not induce excessive pre-stress in the material.

Sensity Tech® technology shows an ability to detect very slight internal material degradation.

An illustration of the results of the monitoring methods implemented by DGA TA is presented below.

A. Post-processed acoustic emission results for the 4 specimens are represented as 3 curves:

- Top curves showing acoustic events over time with the superposition of traction cycles.

- Middle curves showing the evolution of Felicity* ratios.

- Bottom curves showing the distribution of acoustic events by energy in green and by number in red, with an arrow for the final rupture zone.

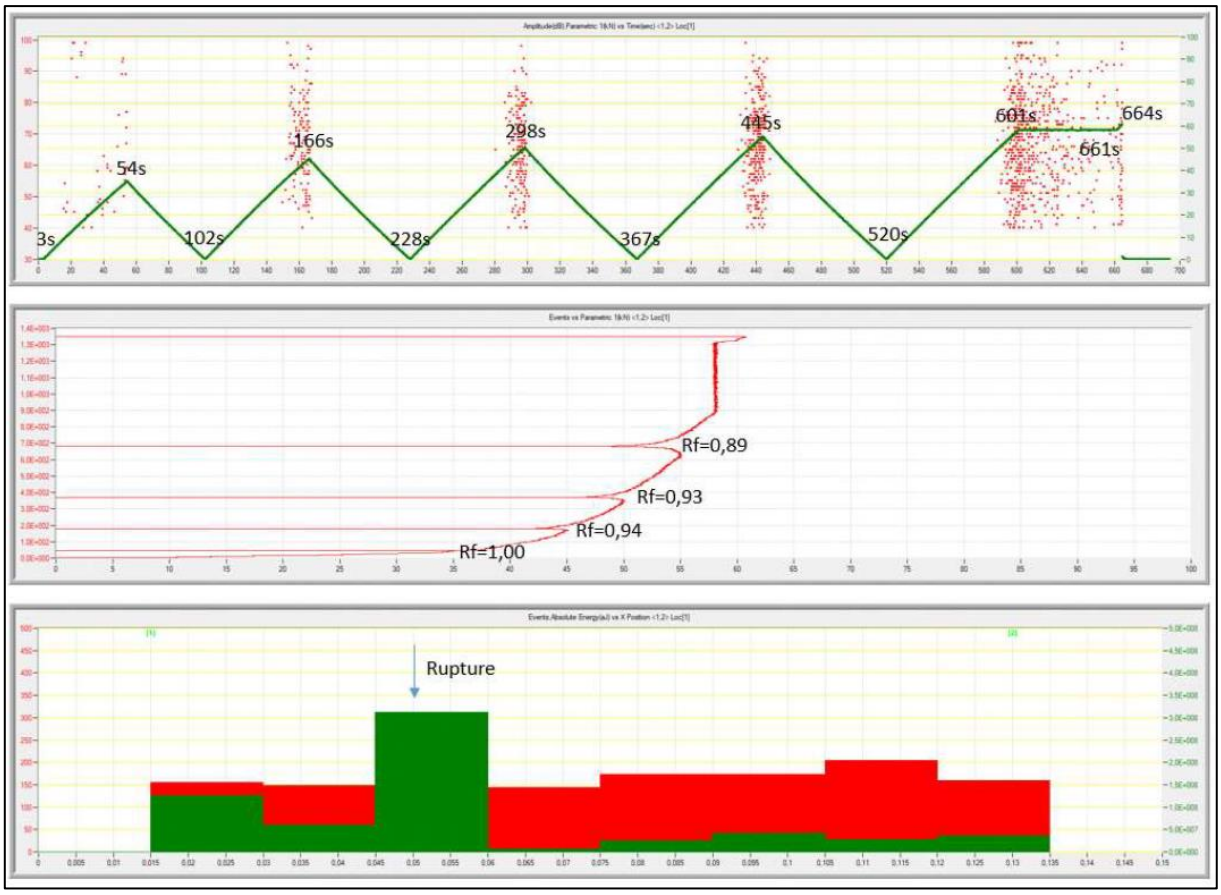

Figure 7: Example of acoustic emission tracking curves

* Definition reminder:

Acoustic Emission generating phenomena are irreversible in nature. The Kaiser effect designates this irreversibility property. If the structure is damaged, the Felicity ratio is less than 1. It is defined as the absence of Acoustic Emission when a material brought to a stress level and then unloaded does not emit as long as the stress applied, during a second loading, remains below the maximum value previously reached.

B. Each stereo-correlation tracking report includes:

- Images of specimen deformation at the beginning of traction and before rupture, with elongation measurements.
- Curves of machine efforts applied over time.
- Curves of elongation measurements in % and specimen deformation during tensile tests.
- Images of specimens after rupture.

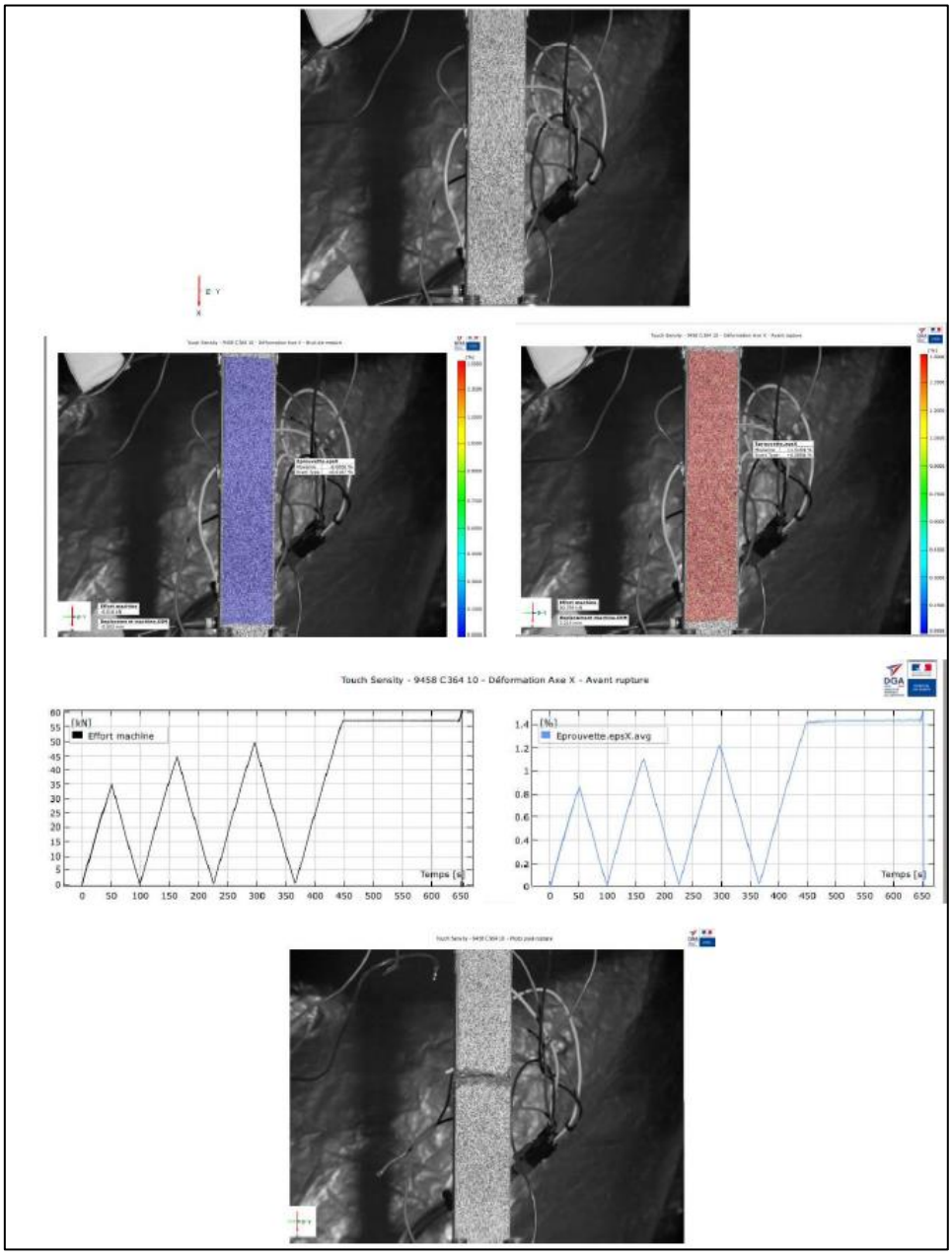

Figure 8: Example of DIC tracking report

C. Each infrared thermography follow-up report includes:

- A software-processed sample image of a specific event identified on the graph below.

- A graph showing the thermal evolution of the six visible connector points in the central area of the samples.

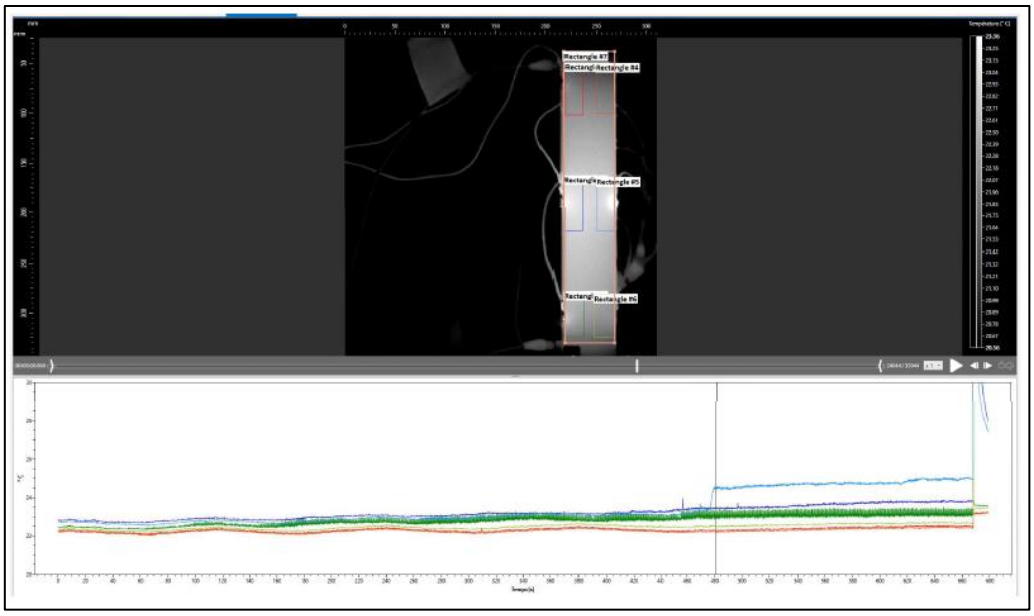

Figure 9: Example of infrared thermography monitoring report

8.1.4. Results Analysis

The results presented below are valid for the majority of the samples tested.

8.1.4.1. Acoustic emission

The results of the acoustic emission monitoring show:

- The Felicity ratios of damage below 1 during the test indicate that irreversible phenomena of the material occur during the tensile cycles.

- The post-processing of the distributions of events in acoustic energy intensity seems consistent on the location of rupture for the specimens but a shift as well as a variation in the intensity of energies at the time of rupture can be observed.

- The distribution of the number of phenomena and their intensity over time shows an increase in density during the cycling peaks, representing a very progressive damage of the specimen.

8.1.4.2. DIC

The analysis of the DIC results does not highlight any precursor phenomenon to specimen failure.

8.1.4.3. Infrared Thermography

The analysis of the results of the infrared thermography monitoring for the specimens shows a constant thermal evolution during the test. Some bursts of thermal intensity representative of carbon fiber breakage on the surface were observed during the tests, but no precursor event to the specimen failure could be identified.

8.1.4.4. Sensitive Tech®

Tracking by the Sensity Tech ® process allows data processing in the form of "raw relative response curves" or in the form of "maps of relative alteration intensity".

** Definition « Raw Relative Response Curve (CRRB) »:

The raw relative response is presented as a time curve allowing to visualize its evolution during the tests. This dimensionless unit of measurement is built directly and instantly from the raw data. Its intensity is absolute and represents the general response of the material through a percentage of variation of its global response compared to a reference state (generally at rest). The higher the raw relative response (RRB), the more the material's response differs from the response it had at rest.

The left curve presented in Figure 10 represents the raw relative response, in the form of a percentage deviation of the specimen's state from its reference state. All internal events are taken into account and interpreted in this case as alterations undergone by the material.

The right curve represent the raw relative responses automatically adapted by Sensity Tech® to the cycling without having data of the loading force. Machine data is shown in orange for comparison.

We can observe a consistency over the periods, peaks of cycling with the % RRB, and stabilizations in plateaus.

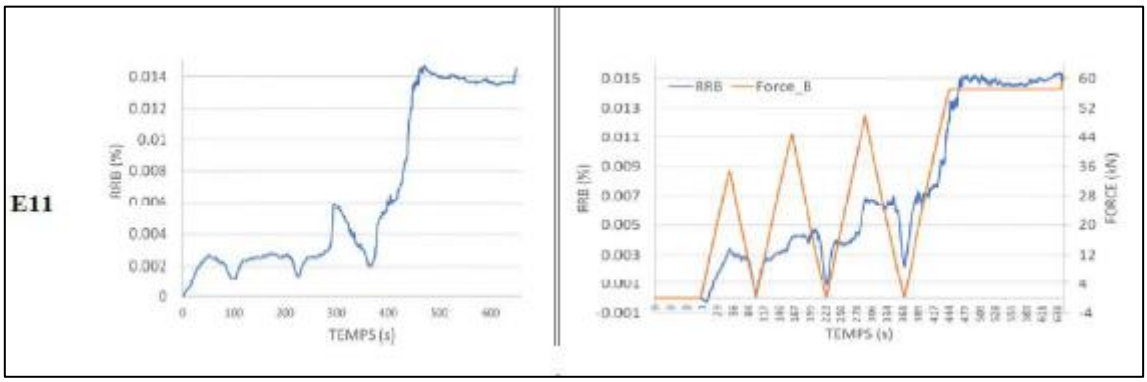

Figure 10: Example of raw response curves

*** Definition « Relative Alteration Intensity Mapping (CIRB) »:

Mapping of the specimen allowing to visualize its internal state and to locate the areas altered compared to the reference state. The Relative Alteration Intensity (IAR) is a dimensionless unit obtained after processing the raw data by the Sensity Tech® algorithms. It quantifies the intensity of alteration undergone by the material compared to a reference state (generally at rest). This dimensionless alteration intensity represents the percentage of local modification in the material's response. The greater this intensity (positive or negative), the more the material's response differs from the response it had at rest. Note that this mapping is much more precise than the previous two because it takes into account all local phenomena within the material.

Figure 11 shows the results on the specimens. These are represented horizontally and the left side corresponds to the upper jaw. The left graphs represent the moments of the traction cycle with the indication of the elongation of the specimens.

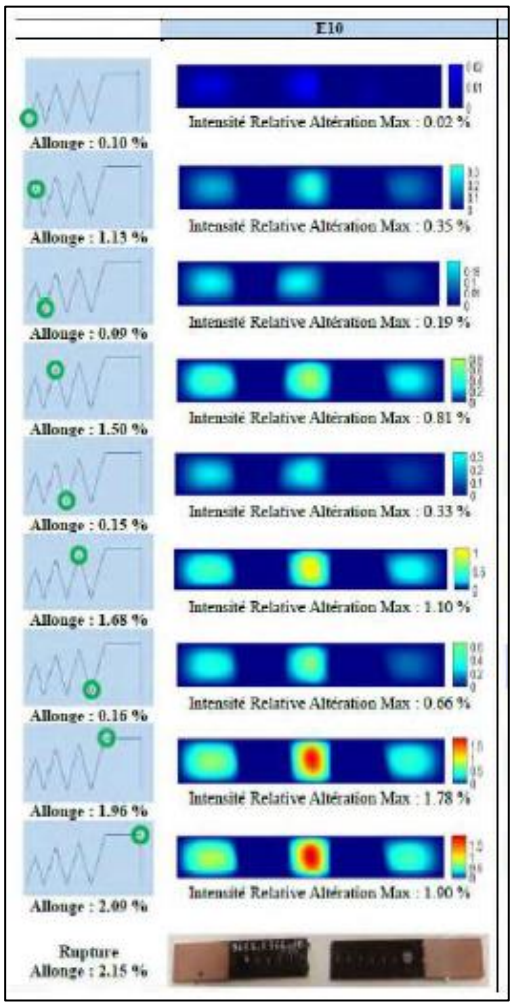

Figure 11: Reconstruction of the internal state by Sensity Tech®: mappings of a tensile test specimen during cycling

8.1.5. Conclusion

These first tests with Sensity Tech® technology have highlighted the ability to detect low-intensity phenomena, including stresses exerted on the specimens during clamping and the initial tensile efforts.

The raw response curves adapted generated by Sensity Tech® technology show a representativeness of the cycles and mechanical regime change phenomena representative as observed on the tensile test specimen compared to the acoustic responses.

Tests confirm that the Sensity Tech® technology allows for mapping representation of all events with highlighting of precursor phenomena of material damage and localization before specimen failure.

8.2. Digital twins for military aircraft: a machine learning approach for monitoring structural ageing

Camille Ferrassou (DGA TA / IMT Toulouse), Paul Escande (IMT Toulouse), Mickaël Duval (DGA TA), Robin Bouclier (IMT Toulouse, ICA, Toulouse) and Laurent Risser (IMT Toulouse)

Unlike civil aviation, where regular maintenance schedules are feasible, military aircrafts are subjected to highly variable flight conditions based on mission requirements.

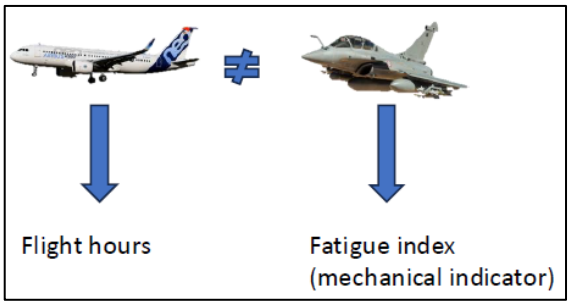

Figure 1: Fleet Fatigue Monitoring

This makes real-time assessment of structural fatigue critical for safety. Traditional approaches rely on physics based models to predict mechanical strains, fatigue, and aging from input flight control data.

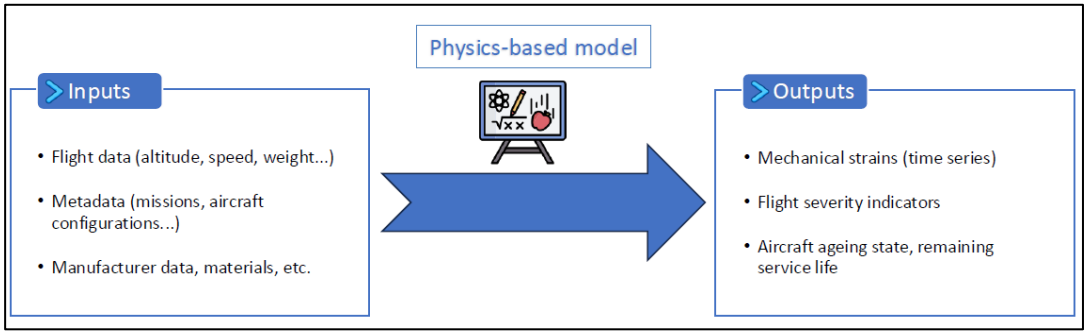

Figure 2: Predicting mechanical ageing: the historical approach

While these models provide significant insights, they may not fully capture the complexities of real-world conditions and can benefit from refinement.

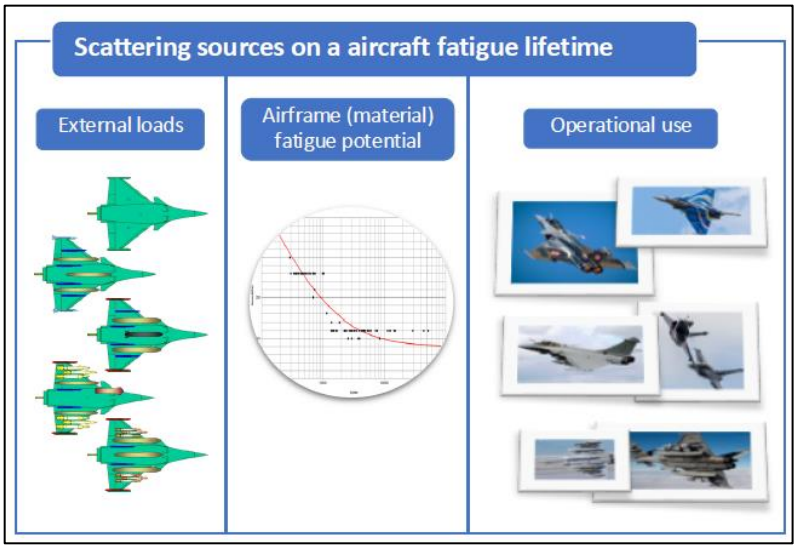

Figure 3: Scattering sources on an aircraft fatigue lifetime

Our research seeks to enhance these models by using machine learning to create digital twins of strain gauges for military aircraft, capable of predicting structural strains and aging based on input-output flight data [1].

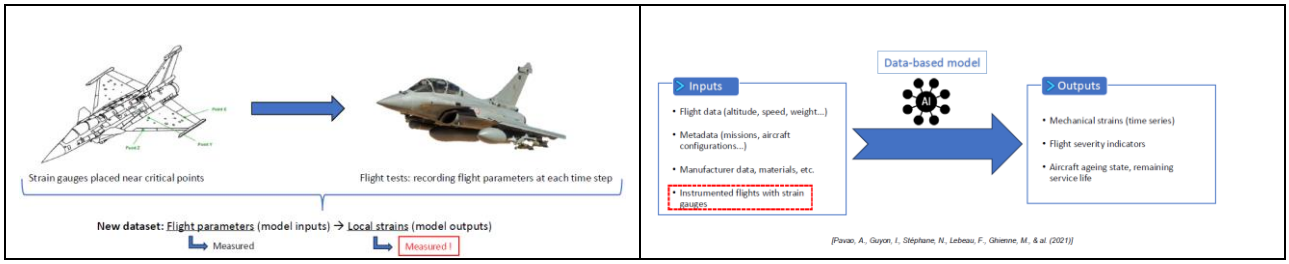

Figure 4: Predicting mechanical ageing: the proposed approach

A part of these flight data, such as altitude, Mach number or others, are routinely measured during flight missions. In this work, structural strains are additionally recorded at critical points on one instrumented aircraft using strain gauges. The objective is then to develop a robust machine learning framework that simulates the behavior of critical aircraft strain gauges under varying operational conditions. In other words, using flight parameters as inputs, we aim to predict the strains experienced at specific points on the aircraft. This predictive capability can improve the planning of maintenance activities, guaranteeing maintenance in operational condition, and therefore enhancing flight safety.

A key step in our project deals with the exploration of the high-dimensional flight data using auto encoders and other techniques, in order to capture complex relationships between flight parameters, reduce the dimensionality of the data, and group similar configurations together.

This reduction is essential for improving the efficiency and accuracy of subsequent regression models, particularly in the context of semi-supervised learning [2], where we leverage both the reconstruction of input data and the prediction of

structural strains to compensate for the lack of labeled data. In this context, we conduct a comparative analysis of various regression models, including tree-based algorithms [3], deep learning models, and semi-supervised approaches [2].

Looking ahead, several key avenues are identified. One important perspective is the incorporation of physics-based insights into the machine learning framework, creating a hybrid model that leverages both data-driven predictions and physical laws [4]. This integration would improve the model's accuracy and its reliability. Additionally, the explainability of the data driven models, using techniques such as LIME (Local Interpretable

Model-agnostic Explanations) or GEMS-AI [5], is crucial. By ensuring transparency in the predictions, we can provide users with the necessary insights to make informed decisions about aircraft maintenance.

[1] Pavao, A., Guyon, I., Stéphane, N. *et al.* Aircraft Numerical "Twin": A Time Series Regression Competition. ICMLA 2021 - 20th IEEE International Conference on Machine Learning and Applications., Dec 2021, Pasadena / Virtual, United States.
[2] Zhang, K., Wen, Q., Zhang, C. *et al.* (2024) Self-Supervised Learning for Time Series Analysis: Taxonomy, Progress, and Prospects, arXiv:2306.10125
[3] Chen, T. and Guestrin C. (2016) XGBoost: A scalable Tree Boostin System. proc KDD, 785-794,
2016
[4] Raissi, M., Perdikaris, P., Karniadakis, G.E. (2019) Physics-informed neural networks: A deep learning framework for solving forward and inverse problems involving nonlinear partial differential equations. Journal of Computational Physics 378, 686-707
[5] Bachoc, F., Gamboa, F., Halford, M., Loubes, J.M., Risser, L. (2023) Entropic Variable Projection for Model Explainability and Interpretability. *Information and Inference: A Journal of the IMA* 12(3); 1686-1715.